LOAN DOCUMENT

PHOTOGRAPH THIS SHEET

DTIC ACCESSION NUMBER

LEVEL

INVENTORY

0

AFRL-ML-TY-TR-1998-4545

DOCUMENT IDENTIFICATION

Oct 98

DISTRIBUTION STATEMENT A

Approved for public release;
Distribution Unlimited

DISTRIBUTION STATEMENT

ACCESSION FOR

NTIS GRA&I ☑

DTIC TRAC ☐

UNANNOUNCED ☐

JUSTIFICATION

BY

DISTRIBUTION/

AVAILABILITY CODES

DISTRIBUTION	AVAILABILITY AND/OR SPECIAL	
A-1		

DISTRIBUTION STAMP

DATE ACCESSIONED

DTIC QUALITY INSPECTED 4

DATE RETURNED

19981118 123

DATE RECEIVED IN DTIC

REGISTERED OR CERTIFIED NUMBER

PHOTOGRAPH THIS SHEET AND RETURN TO DTIC-FDAC

HANDLE WITH CARE

DTIC FORM 70A JUN 90

DOCUMENT PROCESSING SHEET

PREVIOUS EDITIONS MAY BE USED UNTIL STOCK IS EXHAUSTED.

LOAN DOCUMENT

AFRL-ML-TY-TR-1998-4545

ATMOSPHERIC CHEMISTRY OF OXYGENATED ORGANIC COMPOUNDS

J.R. WELLS
J. STEVEN BAXLEY
S.E. WYATT
S.J. MARKGRAF

AFRL/MLQR
139 BARNES DRIVE, STE 2
TYNDALL AFB FL 32403-5323

Approved for public release; Distribution unlimited.

AIR FORCE RESEARCH LABORATORY
MATERIALS & MANUFACTURING DIRECTORATE
AIRBASE & ENVIRONMENTAL TECHNOLOGY DIVISION
TYNDALL AFB FL 32403-5323

NOTICES

WHEN GOVERNMENT DRAWINGS, SPECIFICATIONS, OR OTHER DATA INCLUDED IN THIS DOCUMENT FOR ANY PURPOSE OTHER THAN GOVERNMENT PROCUREMENT DOES NOT IN ANY WAY OBLIGATE THE US GOVERNMENT. THE FACT THAT THE GOVERNMENT FORMULATED OR SUPPLIED THE DRAWINGS, SPECIFICATIONS, OR OTHER DATA DOES NOT LICENSE THE HOLDER OR ANY OTHER PERSON OR CORPORATION, OR CONVEY ANY RIGHTS OR PERMISSION TO MANUFACTURE, USE, OR SELL ANY PATENTED INVENTION THAT MAY RELATE TO THEM.

THIS REPORT IS RELEASABLE TO THE NATIONAL TECHNICAL INFORMATION SERVICE (NTIS). AT NTIS, IT WILL BE AVAILABLE TO THE GENERAL PUBLIC, INCLUDING FOREIGN NATIONS.

THIS TECHNICAL REPORT HAS BEEN REVIEWED AND IS APPROVED FOR PUBLICATION.

J. R. WELLS
Program Manager

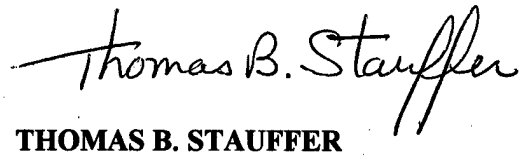

THOMAS B. STAUFFER
Chief, Environmental Technology Development Branch

ANDREW D. POULIS
Scientific & Technical
Information Program Manager

NEIL J. LAMB, Col, USAF, BSC
Chief, Airbase & Environmental Technology Division

IF YOUR ADDRESS HAS CHANGED, IF YOU WISH TO BE REMOVED FROM OUR MAILING LIST, OR IF THE ADDRESSEE IS NO LONGER EMPLOYED BY YOUR ORGANIZATION, PLEASE NOTIFY AFRL/MLQP, TYNDALL AFB, FLORIDA 32403-5323, TO HELP MAINTAIN A CURRENT MAILING LIST.

Do not return copies of this report unless contractual obligations or notice on a specific document requires its return.

REPORT DOCUMENTATION PAGE

Form Approved
OMB No. 0704-0188

1. AGENCY USE ONLY *(Leave blank)*	2. REPORT DATE	3. REPORT TYPE AND DATES COVERED
	22 October 98	Final Report: October 95 - September 98

4. TITLE AND SUBTITLE
Atmospheric Chemistry of Oxygenated Organic Compounds

5. FUNDING NUMBERS

6. AUTHOR(S)
Wells, J.R.; Baxley, J. Steven; Wyatt, S.E.; Markgraf, S.J.

7. PERFORMING ORGANIZATION NAME(S) AND ADDRESS(ES)
AFRL/MLQR
139 Barnes Drive, Ste 2
Tyndall AFB FL 32403-5323

8. PERFORMING ORGANIZATION REPORT NUMBER

9. SPONSORING/MONITORING AGENCY NAME(S) AND ADDRESS(ES)

10. SPONSORING/MONITORING AGENCY REPORT NUMBER
AFRL-ML-TY-TR-1998-4545

11. SUPPLEMENTARY NOTES
Project Officer: R.J. Wells, AFRL/MLQR (850) 283-6087 or DSN 523-6087

12a. DISTRIBUTION AVAILABILITY STATEMENT
Approved for public release; Distribution unlimited.
(PA Case File # 98-451)

12b. DISTRIBUTION CODE
A

13. ABSTRACT *(Maximum 200 words)*

The newly revised ozone and particulate matter regulations will impact decisions on chemical substitution and formulation selection for the Air Force and DoD. Removal of toxic organics and halogenated organics from formulations has been the primary method to meet these new regulatory burdens. However, the substitutes which consist mainly of oxygenated organic compounds (alcohol, aldehydes, ketones and acetates) have poorly understood environmental impacts. To bridge this knowledge gap, investigations into the atmospheric chemistry of this uselful class of compounds has begun. New information presented in this report demonstrates the wide variety of rate constants and transformation mechanisms observed. It was also observed that certain molecular structures enhance hydroxyl radical reactions. This data is important for improving the air quality assessments of new substitutes and formulations and minimizing regulatory constraints.

14. SUBJECT TERMS
hydroxyl radical, atmospheric chemistry, reaction mechanisms, kinetics, ozone, volatile organic compounds, VOC, OH, tropospheric chemistry

15. NUMBER OF PAGES
93

16. PRICE CODE

17. SECURITY CLASSIFICATION OF REPORT	18. SECURITY CLASSIFICATION OF THIS PAGE	19. SECURITY CLASSIFICATION OF ABSTRACT	20. LIMITATION OF ABSTRACT
Unclassified	Unclassified	Unclassified	UL

CLASSIFIED BY:

DECLASSIFY ON:

PREFACE

This report was prepared by the Air Force Research Laboratory's Air Base and Environmental Technology Division of the Materials and Manufacturing Directorate, 139 Barnes Drive, Suite 2, Tyndall AFB, FL 32403-5323, as part of the requirements of F-08637-93-C0020.

EXECUTIVE SUMMARY

A. OBJECTIVE

The objective of this research effort was to determine the atmospheric impact of current and future chemicals used in Air Force coatings systems, coating strippers, cleaners and fuels. Understanding the detailed atmospheric chemistry of these high volume chemicals affords prudent selection and substitution to meet pollution prevention initiatives.

B. BACKGROUND

The Air Force must comply with Clean Air Act Amendments and preceding legislation. The newly revised tighter air quality regulations for particulate matter and regional ozone have emphasized the need to characterize emissions of painting, depainting, cleaning, fueling and other operations. Formulations used by the Air Force are significant sources of uncharacterized volatile organic compounds (VOC) emissions. Currently, Material Safety Data Sheets (MSDS) do not provide the data necessary to assess presently used and potential substitute formulations. Preventing unforeseen regulatory burdens will become more important as decisions are made for new substitutes and new regulations are implemented. Therefore, a detailed understanding of the atmospheric impact of Air Force operations is vital in preventing costly fines and in preventing further pollution of the atmosphere. VOCs have been shown to be involved in the production of tropospheric ozone (O_3) and particulate matter, regulated pollutants. VOCs and their reaction products could also be toxic. Since the detailed atmospheric chemistry of several of these chemicals has never been investigated, experimental atmospheric research is useful to more accurately assess the atmospheric impact of formulation emissions. The information generated by this research will be used to help the Air Force select the most "atmospherically benign" chemicals.

C. SCOPE

The following volatile organic compounds were studied:

Ethyl 3-ethoxypropionate
2-Butoxyethanol
2-Ethoxyethanol
2-Propoxyethanol
2-Butanol
2-Pentanol
isobutyl acetate
hexyl acetate
methyl isobutyrate
hexamethyldisiloxane
octamethyltrisiloxane
decamethyltetrasiloxane

During the study, samples of the volatile organic compounds (VOCs) were subjected to OH radical reactions in simulated atmospheric conditions. To accomplish the project objectives, the following tasks were completed:

1. Development of better analytical methods for collecting and analyzing VOCs and their atmospheric transformation products.

2. Fabrication of small Teflon chamber (30-100 liters) housing.

3. Acquisition of new analytical equipment for better sample collection and definitive transformation product identification.

D. METHODOLOGY

The atmospheric fate of the target VOC was studied under simulated atmospheric (tropospheric) conditions. Hydroxyl radicals (OH) were generated from the photolysis of methyl nitrite (CH_3ONO) in the presence of NO_x. The relative rate technique was used to measure the OH/VOC reaction rate constant. The established reaction rate constant of a reference VOC was used to determine the unknown VOD reaction rate constant. The products of the OH/VOC reaction were monitored by gas chromatography, high pressure liquid chromatography, ion chromatography and mass spectrometry.

E. TEST DESCRIPTION

The VOCs were investigated under simulated atmospheric (tropospheric) conditions. The VOCs were tested for possible photolysis, OH reaction rate constant, and atmospheric transformation products.

F. RESULTS

The following summarizes the results for the laboratory investigations:

1. The rate constants of most of the solvents investigated are consistent with calculated rate constants incorporating structural reactivity concepts.

2. Methylene carbons next to ether oxygens are more likely to be hydroxyl radical hydrogen abstraction sites.

3. Most of the transformation products observed were aldehydes or ketones.

4. The atmospheric transformation mechanisms of VOCs are complex; reaction products consist of several unusual oxygenated organic compounds.

G. CONCLUSIONS

Several of the chemicals investigated are potential solvent substitutes and are in the class of oxygenated organic compounds. Several of the VOCs have never been investigated before and the data generated is useful for modelers to predict air quality impacts. There are still several significant gaps in the detailed knowledge of the atmospheric chemistries of VOC and further research is needed to verify assumptions used in reactivity (ground level ozone potential) models.

H. RECOMMENDATIONS

Determining the OH kinetics, OH + VOC reaction products, and developing more realistic VOC atmospheric reaction mechanisms are areas that continue to need research emphasis. The fruits of this research will benefit the Air Force in at least two ways:

1. Provide avenues of chemical design to build a good solvent with "atmospherically benign" properties.

2. Develop methods to maintain compliance and prevent costly (time and money) fines by intelligent emission practices.

TABLE OF CONTENTS

LIST OF FIGURES

FIGURE TITLE PAGE

LIST OF TABLES

SECTION I

INTRODUCTION

A. OBJECTIVE

The objective of this research project is to determine the atmospheric photochemical reactivity of volatile organic chemicals in present or future use by the US Air Force. This information will be used to assess the environmental impact of formulation emissions. Vapor recovery and scrubbing devices are costly. The type of scientific information gained from this study will provide a basis for cost-effective environmental control strategies consistent with federal, state, and local regulations dealing with air quality controls.

The volatile organic compound (VOC) concentrations and identifications were determined from analysis of coating emissions. This information was coupled with each VOC's incremental reactivity value, tendency to produce ozone (O_3), yielding a basis for assessing each coating system. Ozone is a regulated pollutant, and while not directly emitted, is formed in the atmosphere as a product of VOC atmospheric oxidation [1]. The Environmental Protection Agency is revising its tropospheric ozone concentration regulation which will most likely increase the number of facilities out of compliance. The research results presented here will aid in the selection of coating system(s) to prevent significant O_3 formation.

B. BACKGROUND

Twenty years ago, the first currently accepted chemical mechanisms to explain the formation of photochemical smog were presented. However, even before these were published, it was recognized that the formation of ozone in urban environments resulted

through a series of branching chain reactions involving hydrocarbons (HCs) and oxides of nitrogen (NO_x). What was not recognized was the crucial role played by the hydroxyl radical (OH) to initiate the photochemical chain. Chain carriers in these mechanisms also included organic peroxide and alkoxy radicals and the hydroperoxyl radical (HO_2). These branching chain reactions serve to regenerate OH, and in the process many organic products are formed, including aldehydes and ketones, peroxyacyl nitrates, organic nitrates and peroxides, and other products. During photooxidation nitric oxide (NO) is converted to nitrogen dioxide (NO_2) which then photolyses to produce ozone (O_3).

In urban environments, oxides of nitrogen (particularly NO) required for these reactions to occur come from combustion primarily from automobile exhaust and power plants. On the other hand, sources of hydrocarbons which contribute to the atmospheric load are varied and numerous. They include automobile emissions, industrial emissions, other fossil fuel combustion, commercial emissions, household use of cleaning agents and solvents, natural emissions, and other sources. Evaluating the contribution of each of these sources to the total hydrocarbon loading in a particular regional area is difficult and is being addressed by the U.S. Environmental Protection Agency. Since much of the volatile organic emissions loading can come from numerous small sources, it has become imperative for local and state governments to regulate many generators of volatile organic emissions.

The US Air Force in the course of its normal, peacetime operations performs many regular activities which result in emission of volatile organic compounds (VOCs). A common maintenance operation is the stripping and repainting of aircraft. This process requires large quantities of organic solvents that evaporate into the atmosphere. The

Department of Defense (DoD) has committed itself to complying with local and state regulation, therefore, the impact of these evaporated solvents must be evaluated. In addition, there is a need for understanding the fundamental effects a VOC has on a local region as well as globally. These effects can be considered by the following series of questions: (1) What is the atmospheric lifetime of the emitted VOC; (2) What are the identities and yields of the products formed during the atmospheric degradation of the VOC; and (3) Is the VOC effective in producing ozone when oxidized in the presence of NO_x (4) Are the VOC and/or its products toxic? The answer to these questions is ultimately grounded in understanding the gas-phase kinetics and mechanisms of these compounds when photooxidized under atmospheric conditions.

The VOCs from these solvents interact with trace chemical species such as OH and NO_3 in the atmosphere. These reactions generate products that can further react generating a host of other chemical species. This series of reactions has been shown to eventually produce ozone and a variety of oxygenated and nitrogenated organic species [1]. Therefore research on the solvents and their interaction with the atmosphere is very useful to determine the environmental impact of a maintenance operation. For the program described in this report, selected VOCs were studied to determine their OH rate constants and the products of the atmospheric reactions.

C. SCOPE/APPROACH

Assessing the atmospheric impact of volatile organic compounds requires a detailed knowledge of its atmospheric chemistry. As discussed in the background section, there are three general areas for study to evaluate the fate of emitted VOCs: (1) The reaction rate of VOC + OH, ozone (O_3), and NO_3, and photolysis; (2) Identification of the mechanistic

pathways and product yields; and (3) The overall potential for the VOC to form ozone under atmospheric conditions. Numerous studies have examined each of these aspects from a wide array of VOCs, although not all aspects have been considered for each compound studied.

In general, kinetic studies are concerned only with the rate of removal of chemical species. Mechanistic studies, on the other hand, are concerned with the identity and yield of products generated during the photochemical degradation. However, once the kinetic studies have been completed (as is often the case) a single process is responsible for a large fraction of the total atmospheric removal. Thus, mechanistic studies are frequently focused on the reactions of a single radical (or photolysis). Removal by the hydroxyl (OH) radical is the predominant path for atmospheric removal of many VOCs, thus most mechanistic studies focus on products generated from reaction by OH.

A number of methods have been used over the years to obtain product information from elementary chemical reactions. These have included both spectroscopic and chromatographic methods. For the VOC transformation mechanisms, a combination gas chromatography/mass spectrometry/fourier transform infrared spectroscopy (GC/MS/FTIR) and high pressure liquid chromatography (HPLC) analytical techniques were implemented.[2]

SECTION II

EXPERIMENTAL

A. HYDROXYL RADICAL GENERATION

Hydroxyl radical are generated in Teflon®-film bags by the photolysis of methyl nitrite in air [3]:

$$CH_3ONO + h\nu \Rightarrow CH_3O + NO \quad (1)$$

$$CH_3O + O_2 \Rightarrow CH_2O + HO_2 \quad (2)$$

$$HO_2 + NO \Rightarrow \mathbf{OH} + NO_2 \quad (3)$$

Methyl nitrite was synthesized by dropwise addition of 50% sulfuric acid into a methanol-saturated solution of sodium nitrite according to the procedure of Taylor *et al.*[4]. The methyl nitrite purity was confirmed by GC/FTIR/MS, collected in a lecture bottle and stored at room temperature.

For the OH kinetic experiments, irradiations are carried out in 30- to 100- liter, 2-mil FEP Teflon® surrounded by black (UV) and actinic lights. The bag and lamps are housed inside a wooden box lined with reflective foil.

B. RELATIVE RATE TECHNIQUE

The relative rate technique is used to measure OH rate constants for the VOCs, investigated [3]. The system schematic is shown in Figure 1. The experiment consists of placing the compound of interest (the sample S), a reference compound (R), and OH source, and an excess of NO into a Teflon® bag. This mixture is then irradiated for specific time intervals. After each irradiation a portion of the contents (50-300 mL) from the Teflon® chamber is collected onto a cryogenically cooled sample loop, flash heated,

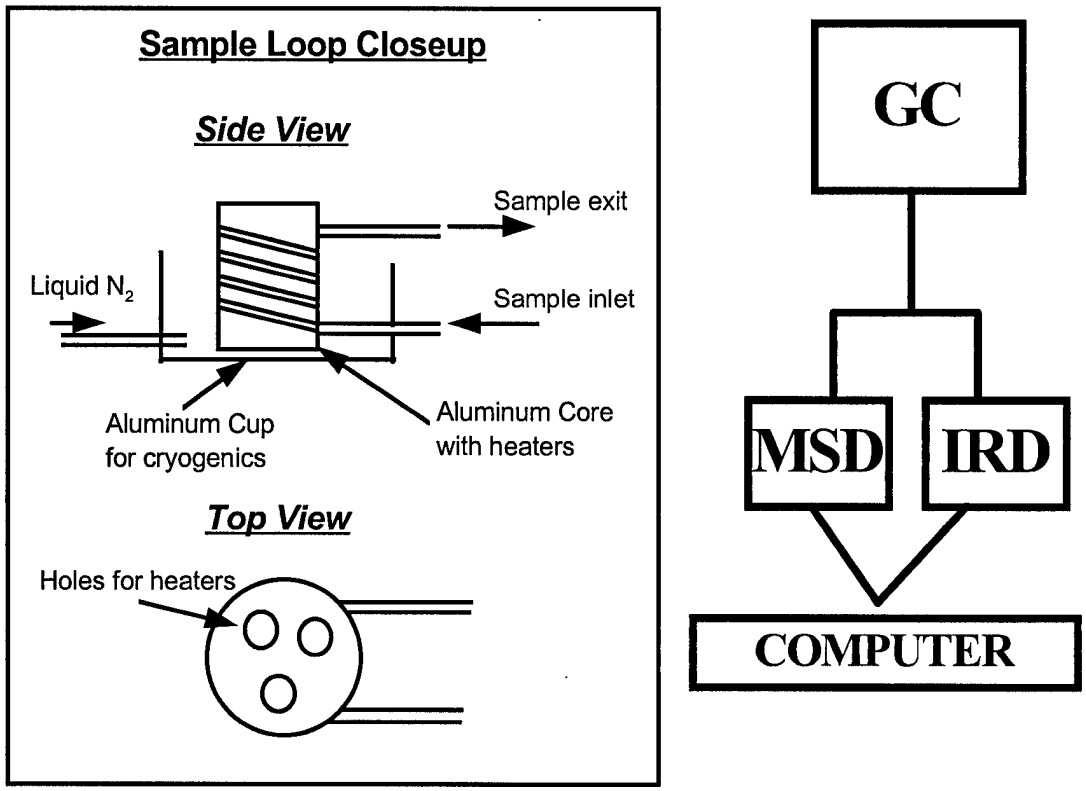

Figure1. The coatings collection apparatus and detail of sample loop. Abbreviations are explained in the text.

and injected onto a gas chromatograph. The concentrations of the reference and the sample compound are used to determine the OH rate constant for the sample compound.

The OH generated by the photolysis of methyl nitrite (CH_3ONO) react with the reference, R, and the sample, S,:

$$OH + S \xrightarrow{k_S} \text{Products} \qquad (4)$$

$$OH + R \xrightarrow{k_R} \text{Products} \qquad (5)$$

Assuming the reaction with OH is the only significant loss process for both the reference and the sample, the rate equations for reactions (4) and (5) are combined and integrated resulting in the following equation:

$$\ln\frac{[S]_0}{[S]_t} = \frac{k_S}{k_R}\ln\frac{[R]_0}{[R]_t} \qquad (6)$$

Where $[X]_0$ refers to the species concentration before OH generation and $[X]_t$ is the species concentration at some arbitrary reaction time, *t*. Plots of $\ln([S]_0/[S]_t)$ versus $\ln([R]_0/[R]_t)$ are linear (see Figures 2 -11) with a slope of k_S/k_R and an intercept of zero. Therefore multiplying the slope of the linear least squares fit of the data by the established rate constant, k_R, yields k_S.

$$k_S = k_R \times \text{slope} \qquad (7)$$

C. VOC EXPERIMENTAL PARAMETERS

1. OH Rate Constant Experiments

A reference compound (1 to 3 ppmv), VOC (1 to 3 ppmv), methyl nitrite (5 to 10 ppmv as the OH source), nitric oxide (NO) (1 to 2.5 ppmv added to support the OH

formation and suppress ozone (O_3) reactions) were mixed for approximately 45 minutes and prephotolysis reactant concentrations ($[S]_0$ and $[R]_0$) are measured. Approximately 50 to 200 milliliters of the chamber contents are sampled by vacuum collection onto a glass-bead-filled sample loop (approximate volume 1.3 mL) cryogenically cooled to a specified temperature, typically -100°C, then flash-heated and injected onto a megabore or capillary gas chromatographic column [2]. The reactant concentrations are measured by gas chromatography (Hewlett-Packard Model 5890 GC) with flame ionization detection (FID). The total irradiation time was kept as short as possible to prevent complications for the reaction products. Each experiment consists of 5 irradiations with the total loss of the sample and reference compounds under 50%. The column choice changes are based on the polarity of the compound of interest, resolution of reference and sample, and resolution of reaction products. Typically, the GC oven temperature is programmed from 35 to 210°C with helium as the carrier gas.

The key assumption of the relative rate technique is the decrease of both the reference and the sample is due solely to reaction with photolytically generated OH. Typical experimental mixtures of methyl nitrite, sample and reference are left in the dark for average experimental period (up to 8 hours). For VOCs investigated there was no observable loss. Each VOC investigated was also exposed to chamber lights to check for photolysis; again, no loss was observed.

Separate experiments in which mixtures of methyl nitrite, NO and sample ***or*** reference are irradiated demonstrate that primary and secondary reaction products do not overlap with the sample or reference gas chromatograph retention times.

2. Product determination

a. Gas chromatography/mass spectrometry/ infrared spectroscopy

Identifying and quantifying the products formed in the OH + VOC reaction are necessary to better understand atmospheric reaction mechanisms. Product identification is also necessary to evaluate the environmental impact of a VOC. The reaction products could be more harmful than the compound of interest.

Product identifications are performed using both the small (30 - 100 L) and large (3,000 L) chambers coupled to a Hewlett-Packard (HP) 5890 II Plus GC equipped with an HP 5965 B Infrared detector (IRD) and an HP 5971 mass selective detector (MSD). The column effluent is split between the HP 5971 and HP 5965 B using a glass capillary "Y" splitter (Restek Corp. and Supelco). This affords the simultaneous mass spectrum detection and infrared spectrum collection of analyte peaks. The IRD collects an IR spectrum every 0.67 seconds (8 cm^{-1} resolution with each four scans (1.5 scans/second) averaged). The MSD collects data in the scan mode at 1.9 scans/second.

The chamber is filled with air, NO (2 to 5 ppmv), methyl nitrite (2 to 5 ppmv) and the VOC of interest (2 to 20 ppmv). The contents are irradiated initiating reactions (1)-(3). The OH reacts with the VOC and products are formed. The chamber contents were analyzed before irradiation to collect a background and analyzed after each subsequent irradiation to monitor VOC loss and product growth.

Approximately 50 to 200 mL of the small *or* large chamber contents are sampled by vacuum collection onto a glass bead filled sample loop (approximate volume 1.3 mL) cryogenically cooled to a specified temperature, typically -100°C, then flash-heated and injected onto a megabore or capillary gas chromatographic column. Helium is used as the carrier gas and the GC oven temperature was ramped from 35 to 220°C.

b. Aldehydes and Ketones

Aldehydes and ketones have similar infrared signatures and are therefore difficult to quantify by FTIR, and they can be difficult to analyze by gas chromatography. An analytical method by which these aldehyde and ketone reaction products are derivitzed to hydrozones and analyzed by high pressure liquid chromatography (HPLC) has been a successful technique [5].

$$R_1\text{-}C(O)\text{-}R_2(H) + H_2N\text{-}N(H)(C_6H_3(NO_2)_2 \Rightarrow H_2O + R_1(R_2)\text{-}C{=}N\text{-}N(H)(C_6H_3(NO_2)_2 \qquad (8)$$

An HP 1050 HPLC is used with a single DuPont Zorbax™ ODS column (25 cm x 46 cm, 5 μm particle size). Methanol and acetonitrile, both HPLC grade, were obtained from Fisher Scientific and used as received. Water was deionized (18 megaohm) using a Milli-Q® system. A 26-minute ternary gradient mobile phase at a constant flow of 1ml/min is used as follows:

Water- 40% decreased linearly to 25% at 10 minutes, further decreased to 15% at 20 minutes and held constant to 26 minutes.

Acetonitrile- 20% decreased linearly to 5% at 10 minutes and held constant to 26 minutes.

Methanol-40% increased linearly to 70% at 10 minutes, further increasing linearly to 80% at 20 minutes, and held constant to 26 minutes.

c. Quantification

Quantification data are used to account for the loss of the sample due to OH/VOC reaction. This information is used to more clearly describe the reaction mechanism. After the products are identified, experiments to measure the loss of VOC and the generation of products are done.

E. INCREMENTAL REACTIVITY

The regulatory agencies are desperate to have a simple, predictable method for determining the ozone forming potential of a given compound released into a polluted atmosphere. This need is hampered by the lack of detailed atmospheric kinetic and mechanistic information for VOC, the lack of detailed knowledge of the pertinent reactive processes and reactive species concentrations, and by the fact that not all VOCs produce the same amount of ozone. Also, the type and concentrations of pollutants (i.e. oxides of nitrogen (NO_x) and other VOCs) that drive the formation of O_3 are different at different times of the day and at different locations. One of the most significant factors for O_3 formation is the [VOC]/[NO_x] ratio [1,6], but in the complex system of the atmosphere there is not a simple relationship correlating the ratio to O_3 concentration. Distillation of all of these atmospheric effects and processes into a simple to understand, single number is a daunting task. But, because this is such an important issue and a best educated guess is better than nothing at all, the California Air Resources Board (CARB) has adopted a model developed by Bill Carter [7] to calculate the incremental reactivity of a VOC. The model calculates, for 119 different base case scenarios, the average amount of O_3 formed when a small amount of a VOC is emitted. This average is a single number called the incremental reactivity. These calculations put each VOC on more equal footing, since not all VOC have the same ozone production potential.

The Maximum Incremental Reactivity (MIR_{VOC}) is currently used as the incremental reactivity metric and is derived by adjusting (mathematically) the NO_x emissions, and hence the [VOC]/[NO_x] ratio, in each base case to yield the highest incremental reactivity.

SECTION III

RESULTS

A. OH RATE CONSTANTS

1. Hydroxyl Radical/EEP Reaction Rate Constant

The OH rate constant for ethyl 3-ethoxypropionate (EEP, CH_3CH_2-O-$CH_2CH_2C(O)O$-CH_2CH_3) was obtained using the relative rate method described above. Typically five experimental runs were conducted on each EEP/reference pair. The plot of a modified version of equation (6) is shown in Figure 2. The $\ln([R]_0/[R]_t)$ term is divided by the respective reference rate constant (dodecane $(14.2 \pm 3.6) \times 10^{-12}$ $cm^3molecule^{-1}s^{-1}$ and n-nonane $(10.2 \pm 2.6) \times 10^{-12}$ $cm^3molecule^{-1}s^{-1}$) [8] and multiplied by 10^{-12} $cm^3molecule^{-1}s^{-1}$ resulting in a unitless number and yielding a slope that is equal to the hydroxyl radical/EEP rate constant, k_{EEP}, *divided by* 10^{-12} $cm^3molecule^{-1}s^{-1}$. This modification allows for a direct comparison to the two reference compound/EEP data sets. The slope of the line yields an hydroxyl radical bimolecular rate constant, k_{EEP}, of $(22.9 \pm 0.8) \times 10^{-12}$ $cm^3molecule^{-1}s^{-1}$. The data points at the origin are experimental points because pre-irradiation, $t = 0$, data showed no detectable loss of EEP or reference. The error in the rate constant stated above is the 95% confidence level from the random uncertainty in the slope. Incorporating the uncertainties associated with the reference rate constants (± 25%) used to derive the EEP/OH rate constant yields a final value for k_{EEP} of $(22.9 \pm 7.4) \times 10^{-12}$ $cm^3molecule^{-1}s^{-1}$. Assuming an $[OH] = 1 \times 10^6$ molecules cm^{-3}, the atmospheric (1/e) lifetime calculated for EEP is 12 hours. The EEP/OH rate constant, k_{EEP}, has not been previously reported. The observed rate constant can be compared with a k_{EEP} calculated using a structure reactivity relationship [9]. The calculated k_{EEP} was

$20 \times 10^{-12} cm^3 molecule^{-1} s^{-1}$, in agreement with our measured value.

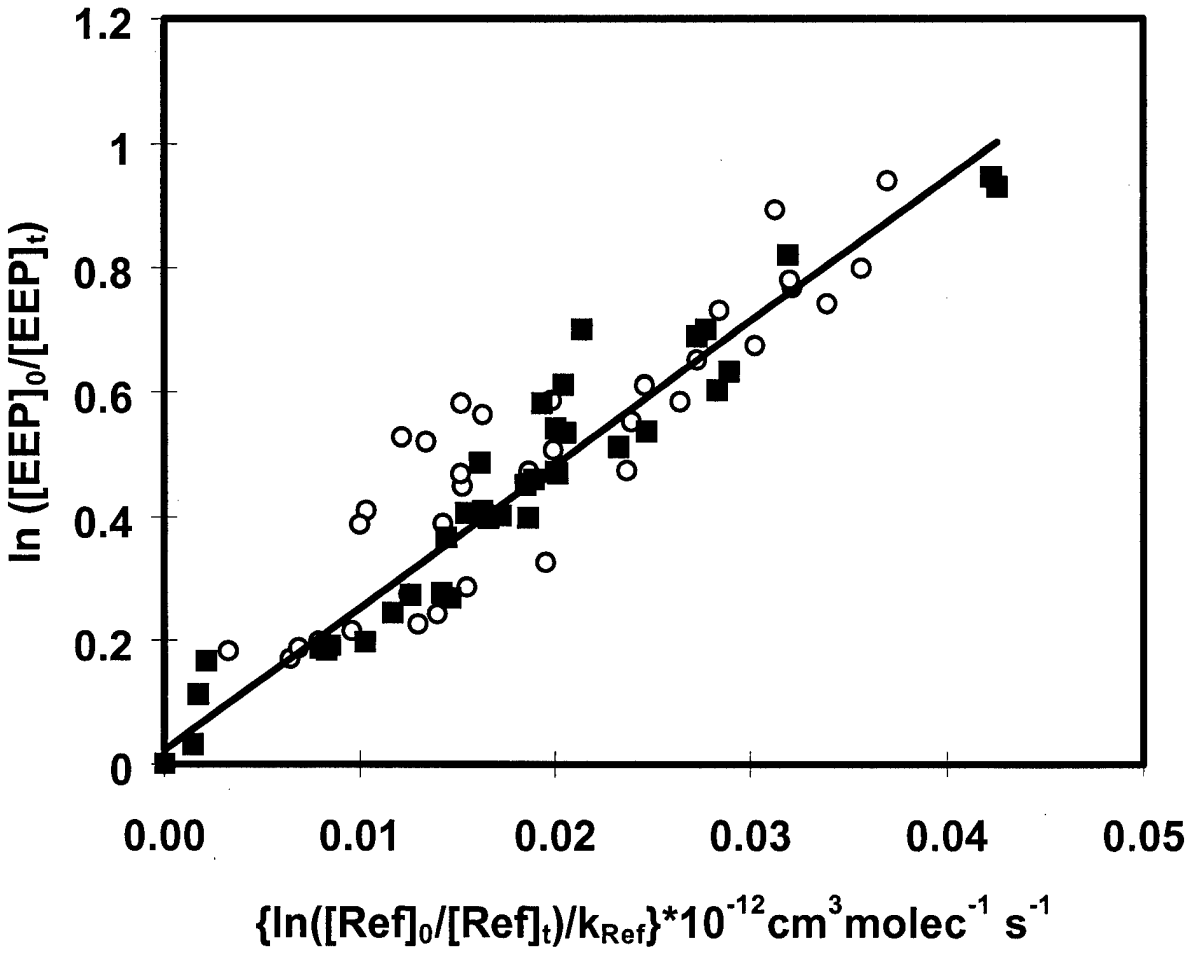

Figure 2. Ethyl 3-ethoxypropionate relative rate plot with both n-nonane and dodecane as reference compounds. The OH + EEP rate constant, k_{EEP}, measured is 22.9 ± 0.8 x 10^{-12} $cm^3molecule^{-1}s^{-1}$. The dodecane as a reference(■) data are overlayed with the n-nonane as a reference (○)data.

2.Hydroxyl Radical/Hydroxy ether Reaction Rate Constant

The OH rate constants for 2-ethoxyethanol (2EEOH, $CH_3CH_2OCH_2CH_2(OH)$) and 2-butoxyethanol (2BEOH, $CH_3CH_2CH_2CH_2OCH_2CH_2(OH)$) were obtained using the relative rate method described above. Typically five experimental runs were conducted on each hydroxy ethers/reference pair. The plots of a modified version of equation (6) are shown in Figures 3(2EEOH) and 4 (2BEOH). The $\ln([reference]_0/[reference]_t)$ term is divided by the respective reference rate constant (dodecane $(14.2 \pm 3.6) \times 10^{-12} cm^3 molecule^{-1} s^{-1}$ and n-nonane $(10.2 \pm 2.6) \times 10^{-12} cm^3 molecule^{-1} s^{-1}$) [8] and multiplied by $10^{-12} cm^3 molecule^{-1} s^{-1}$ resulting in a unitless number and yielding a slope that is equal to the hydroxyl radical/hydroxy ether rate constant, $k_{hydroxy\ ether}$, *divided by* $10^{-12} cm^3 molecule^{-1} s^{-1}$. This modification allows simultaneous comparison of the two reference compound/hydroxy ether data sets.

a. Hydroxyl Radical/Hydroxy ether Reaction Rate Constant (k_{2EEOH}, k_{2BEOH})

The slopes of the line in Figures 3 and 4 yields hydroxyl radical bimolecular rate constants of $(15.8 \pm 1.1) \times 10^{-12} cm^3 molecule^{-1} s^{-1}$ and $(22.5 \pm 0.7) \times 10^{-12} cm^3 molecule^{-1} s^{-1}$ for 2-ethoxyethanol, k_{2EEOH}, and 2-butoxyethanol, k_{2BEOH}, respectively. The data points at the origin are experimental points because pre-irradiation, t = 0, data showed no detectable loss of 2EEOH, 2BEOH or references. The error in the rate constant stated above is the 95% confidence level from the random uncertainty in the slope. Incorporating the uncertainties associated with the reference rate constants (± 25%) used yields a final value for k_{2EEOH} of $(15.8 \pm 3.8) \times 10^{-12} cm^3 molecule^{-1} s^{-1}$ and k_{2BEOH} of $(22.5 \pm 5.6) \times 10^{-12} cm^3 molecule^{-1} s^{-1}$. Assuming an $[OH] = 1 \times 10^6$ molecules cm^{-3}, the

atmospheric (1/e) lifetimes calculated for 2EEOH and 2BEOH are 18 and 12 hours, respectively. The 2EEOH/OH rate constant, k_{2EEOH}, has been previously measured by Dagaut *et al.*(via relative rate $18.7 \pm 2.0 \times 10^{-12}$cm^{3}molecule^{-1}s^{-1}) [10], Stemmler *et al.* (via relative rate $(14.5 \pm 0.4) \times 10^{-12}$cm^{3}molecule^{-1}s^{-1})[11,12], Porter *et al.* (via relative rate (17.4 ± 3.1) and via pulsed laser photolysis-laser-induced fluorescence $(21.2 \pm 0.7) \times 10^{-12}$cm^{3}molecule^{-1}s^{-1})[6] and Hartman *et al.* (via laser photolysis resonance fluorescence $(12 \pm 3) \times 10^{-12}$cm^{3}molecule^{-1}s^{-1}) [13]. The 2BEOH/OH rate constant, k_{2BEOH}, has been previously measured by Dagaut *et al.*(via relative rate $(23.1 \pm 0.9) \times 10^{-12}$cm^{3}molecule^{-1}s^{-1})[10] , Stemmler *et al.* (via relative rate $(19.4 \pm 2.0) \times 10^{-12}$cm^{3}molecule^{-1}s^{-1}) [12,14], Hartman *et al.* (via laser photolysis resonance fluorescence $(14 \pm 3) \times 10^{-12}$cm^{3}molecule^{-1}s^{-1}) [13]and Aschmann *et al.* (via relative rate $(29.4 \pm 4.3) \times 10^{-12}$cm^{3}molecule^{-1}s^{-1}) [15] and other than Hartmann *et al.* [5] are consistent with the value reported here($(22.5 \pm 5.6) \times 10^{-12}$cm^{3}molecule^{-1}s^{-1}). Using structure reactivity, k_{2EEOH} and k_{2BEOH} values of 22×10^{-12}cm^{3}molecule^{-1}s^{-1} and 26×10^{-12}cm^{3}molecule^{-1}s^{-1}, respectively were calculated. [9]

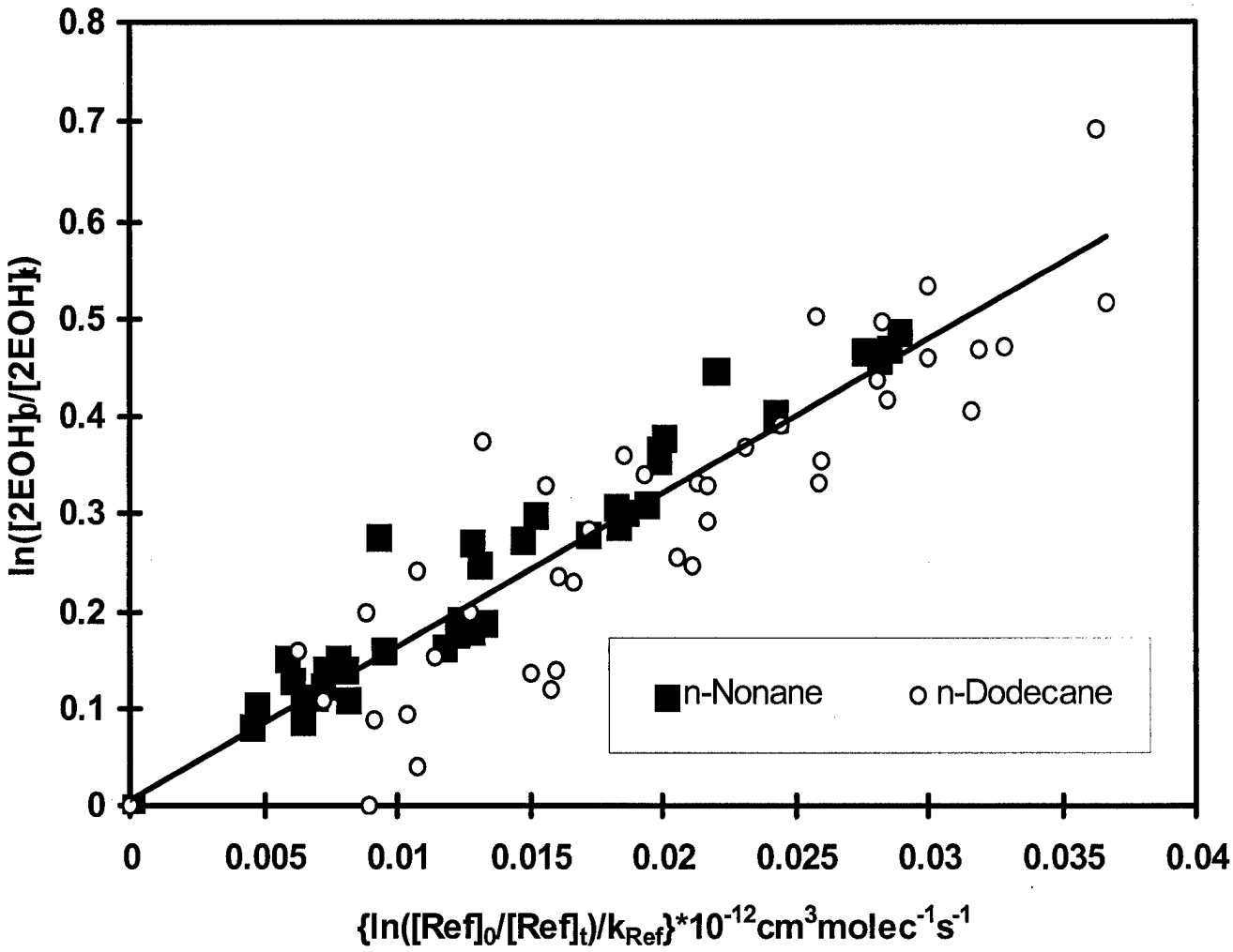

Figure 3. Relative rate data for 2-ethoxyethanol with both n-nonane (■) and dodecane (O) as reference compounds. The OH + 2EEOOH rate constant, k_{2EEOH}, measured is 15.8 ± 1.1 x 10^{-12} $cm^3molecule^{-1}s^{-1}$.

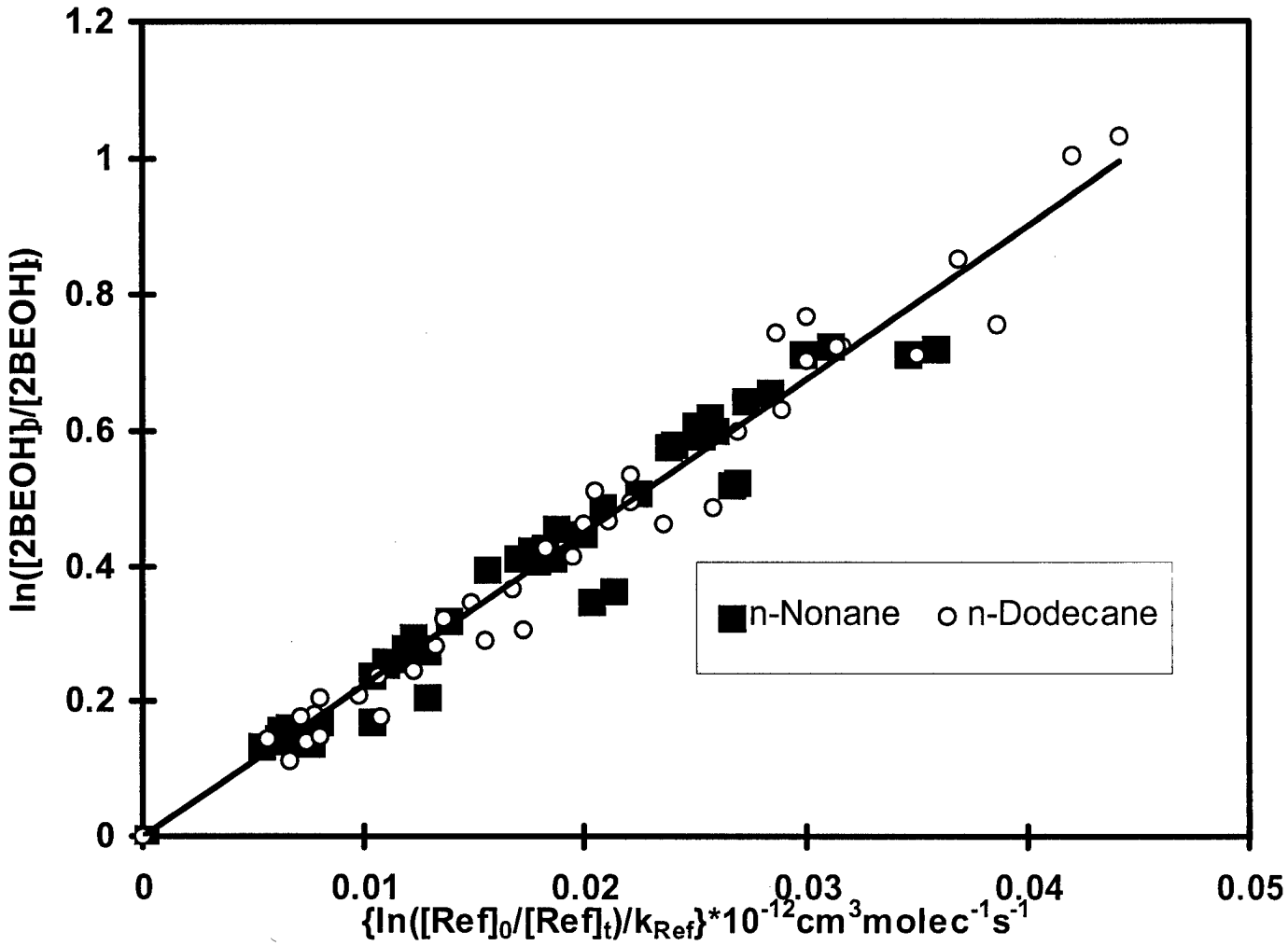

Figure 4. Relative rate data for 2-butoxyethanol with both n-nonane (■) and dodecane (O) as reference compounds. The OH + 2BEOH rate constant, k_{2BEOH}, measured is 22.5 ± 0.7 x 10^{-12} $cm^3molecule^{-1}s^{-1}$.

3. Hydroxyl Radical/2-Propoxyethanol Reaction Rate Constant (k_{2PEOH})

The OH rate constant for 2-propoxyethanol (2PEOH, $CH_3CH_2CH_2OCH_2CH_2(OH)$) was obtained using the relative rate method described above. Typically five experimental runs were conducted on each 2PEOH/reference pair. The plots of a modified version of equation (6) are shown in Figure 5. The $\ln([reference]_0/[reference]_t)$ term is divided by the respective reference rate constant (2-pentanone $(4.9 \pm 1.2) \times 10^{-12}cm^3molecule^{-1}s^{-1}$ and n-octane $(8.7 \pm 2.2) \times 10^{-12}cm^3molecule^{-1}s^{-1}$) [8] and multiplied by $10^{-12}cm^3molecule^{-1}s^{-1}$ resulting in a unitless number and yielding a slope that is equal to the hydroxyl radical/2PEOH rate constant, k_{2PEOH}, *divided by* $10^{-12}cm^3molecule^{-1}s^{-1}$. This modification allows simultaneous comparison of the two reference compound/ 2PEOH data sets.

The slope of the line in Figure 5 yields hydroxyl radical bimolecular rate $(21.4 \pm 1.3) \times 10^{-12}cm^3molecule^{-1}s^{-1}$ for 2-propoxyethanol, k_{2PEOH}. The data points at the origin are experimental points because pre-irradiation, t = 0, data showed no detectable loss of 2PEOH or references. The error in the rate constant stated above is the 95% confidence level from the random uncertainty in the slope. Incorporating the uncertainties associated with the reference rate constants (average uncertainty ± 25%) used yields a final value for k_{2PEOH} of $(21 \pm 6) \times 10^{-12}cm^3molecule^{-1}s^{-1}$. Assuming an $[OH] = 1 \times 10^6$ molecules cm^{-3}, the atmospheric (1/e) lifetimes calculated for 2PEOH is 13 hours. The 2PEOH/OH rate constant, k_{2PEOH}, has been previously measured by Stemmler *et al.* (via relative rate $(16.4 \pm 0.7) \times 10^{-12}cm^3molecule^{-1}s^{-1}$)[12]. Using structure reactivity, a k_{2PEOH} value of $25 \times 10^{-12}cm^3molecule^{-1}s^{-1}$ was calculated. [9]

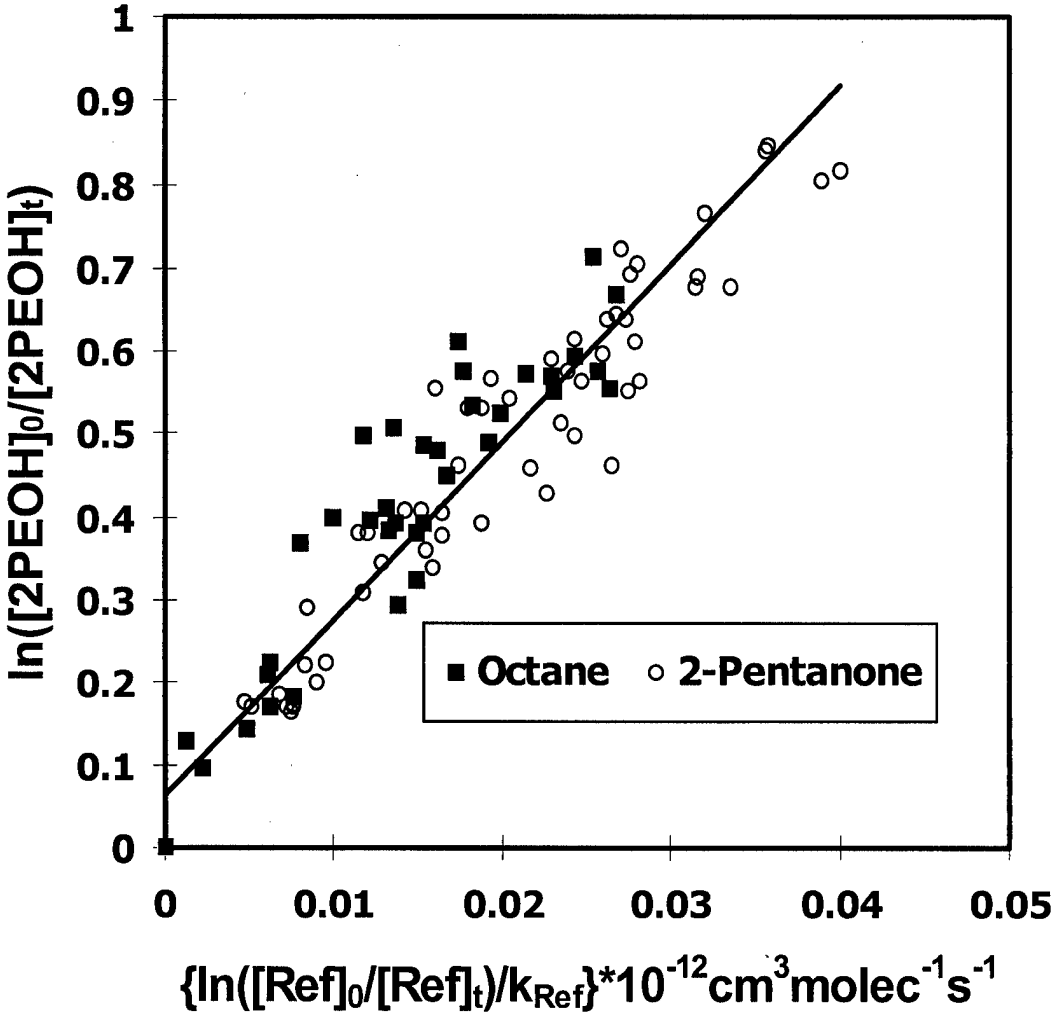

Figure 5. Relative rate data for 2-propoxyethanol with both octane (■) and 2-pentanone (O) as reference compounds. The OH + 2PEOH rate constant, k_{2PEOH}, measured is 21.4 ± 1.3 x 10^{-12} $cm^3molecule^{-1}s^{-1}$.

4. Hydroxyl Radical/Secondary Alcohol Reaction Rate Constant (k_{2BU}, k_{2PE})

The OH rate constants for 2-butanol (2BU, $CH_3CH_2CH(OH)CH_3$) and 2-pentanol (2PE, $CH_3CH_2CH_2CH(OH)CH_3$) were obtained using the relative rate method described above. Typically five experimental runs were conducted on each alcohol/reference pair. The plots of a modified version of equation (6) are shown in Figures 6 (2BU) and 7 (2PE). The $\ln([alcohol]_0/[alcohol]_t)$ term is multiplied by the respective recommended reference rate constant (dodecane $(14.2 \pm 3.6) \times 10^{-12}$ $cm^3molecule^{-1}s^{-1}$ and n-nonane $(10.2 \pm 2.6) \times 10^{-12}$ $cm^3molecule^{-1}s^{-1}$ and heptane $(7.15 \pm 1.79) \times 10^{-12}$ $cm^3molecule^{-1}s^{-1}$) [8] and divided by 10^{-12} $cm^3molecule^{-1}s^{-1}$ resulting in a unitless number and yielding a slope that is equal to the hydroxyl radical/alcohol rate constant, $k_{alcohol}$, *divided by* 10^{-12} $cm^3molecule^{-1}s^{-1}$. This modification allows for simultaneous comparison of the two reference compound/alcohol data sets to demonstrate data consistency.

The individual alcohol/reference data sets yielded the following hydroxyl radical rate constant results: 2-butanol/n-nonane = $(9.26 \pm 0.14) \times 10^{-12}$ $cm^3molecule^{-1}s^{-1}$, 2-butanol/dodecane = $(8.14 \pm 0.47) \times 10^{-12}$ $cm^3molecule^{-1}s^{-1}$, 2-pentanol/heptane = $(9.93 \pm 1.21) \times 10^{-12}$ $cm^3molecule^{-1}s^{-1}$, and 2-pentanol/dodecane = $(12.46 \pm 0.88) \times 10^{-12}$ $cm^3molecule^{-1}s^{-1}$. The combination of both alcohol/reference data sets are shown in Figures 6(2BU) and 7 (2PE). The slopes of the lines in Figures 6 and 7 yield an hydroxyl radical bimolecular rate constants of $(8.09 \pm 0.36) \times 10^{-12}$ $cm^3molecule^{-1}s^{-1}$ and $(11.89 \pm 0.66) \times 10^{-12}$ $cm^3molecule^{-1}s^{-1}$ for 2-butanol, k_{2BU}, and for 2-pentanol, k_{2PE}, respectively. The data points at the origin are experimental points because pre-irradiation, t = 0, data showed no detectable loss of 2BU, 2PE or references. The error in the rate constant stated above is the 95% confidence level from the random uncertainty in the slope. Incorporating the uncertainties associated with the reference rate constants used (± 25%)

yields final values for k_{2BU} of (8.1 ± 2.0) x 10^{-12} $cm^3molecule^{-1}s^{-1}$ and k_{2PE} of (11.9 ± 3.0) x 10^{-12} $cm^3molecule^{-1}s^{-1}$ which are within experimental error of the individual alcohol/reference data set results. Assuming an OH concentration of 1 x 10^6 molecules cm^{-3}, the atmospheric (1/e) lifetimes calculated for 2BU and 2PE are 34 and 23 hours, respectively. The 2BU/OH rate constant, k_{2BU}, has been previously measured, using the relative rate method, by Chew *et al.* [16] yielding a value of (9.2 ± 2.4) x 10^{-12} $cm^3molecule^{-1}s^{-1}$, within error limits of our reported value. Wallington *et al.*,using flash photolysis resonance fluorescence, reported a k_{2PE} of (11.8 ± 0.8) x 10^{-12} $cm^3molecule^{-1}s^{-1}$, also within error limits of our reported value [17]. Using structure reactivity, the calculated k_{2BU} of 9.8 x 10^{-12} $cm^3molecule^{-1}s^{-1}$ and k_{2PE} of 11 x 10^{-12} $cm^3molecule^{-1}s^{-1}$ are within error limits of our and the previously reported values. [9]

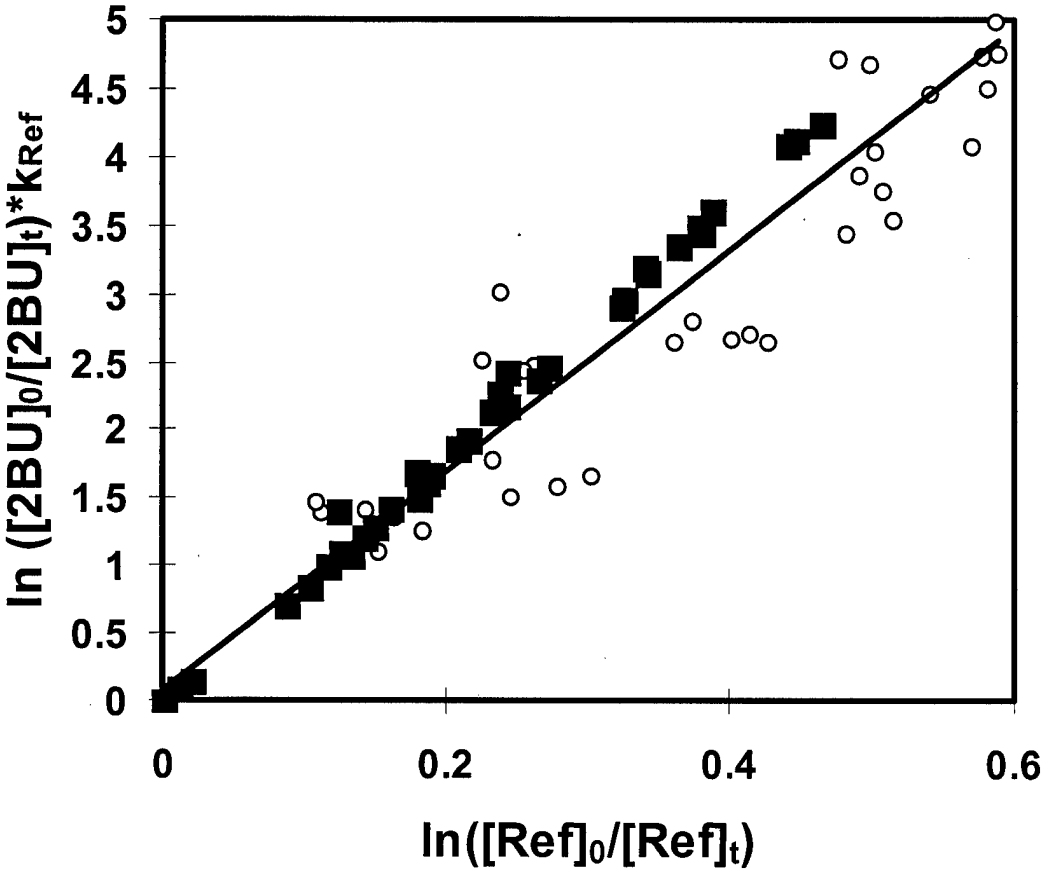

Figure 6. Relative rate data for 2 butanol with both n-nonane (■) and dodecane (O) as reference compounds. The OH + 2BU rate constant, k_{2BU}, measured is (8.09 ± 0.36) x 10^{-12} $cm^3molecule^{-1}s^{-1}$.

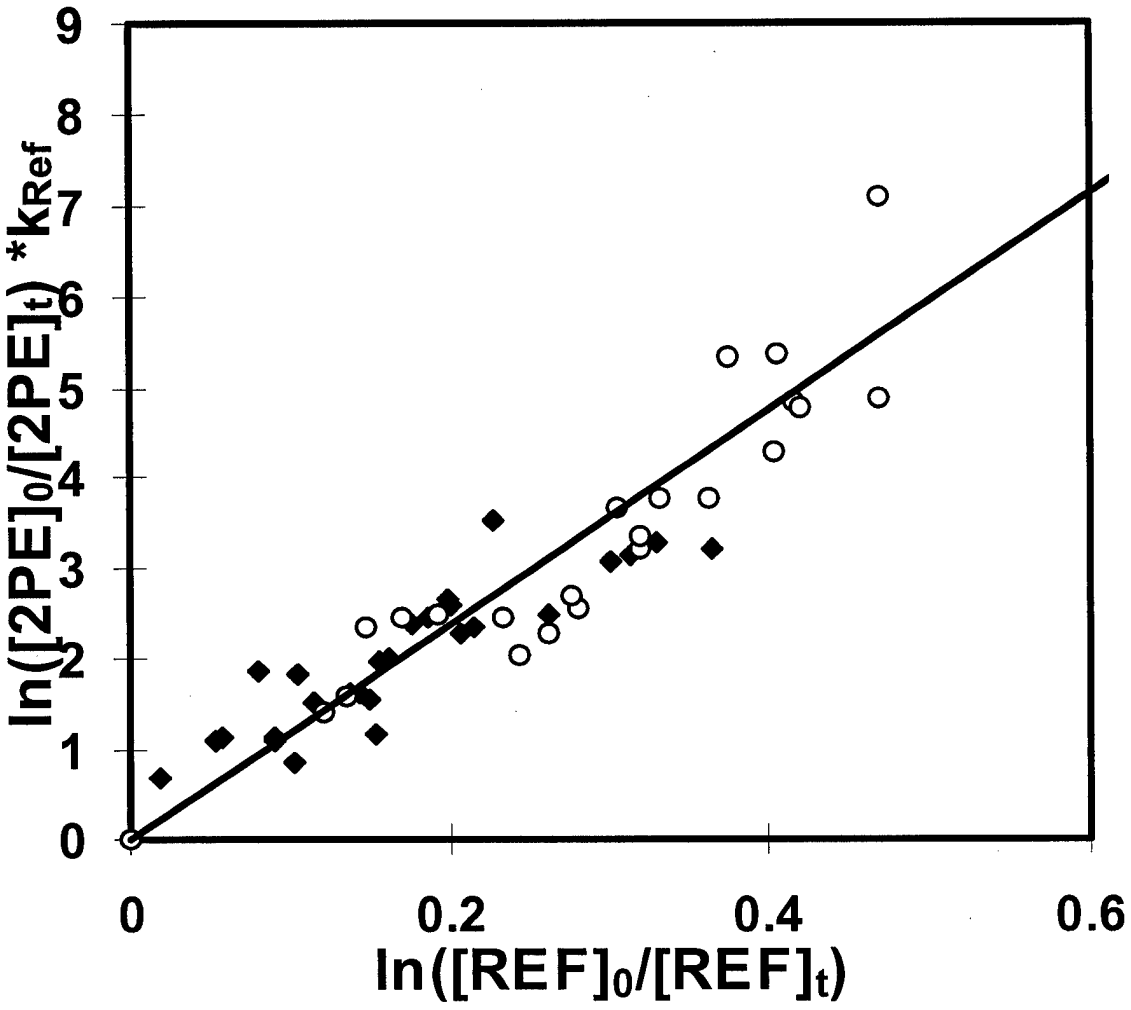

Figure 7. Relative rate data for 2 pentanol with both heptane (◆) and dodecane (O) as reference compounds. The OH + 2PE rate constant, k_{2PE}, measured is (11.89 ± 0.66) x 10^{-12} $cm^3molecule^{-1}s^{-1}$.

5. Hydroxyl Radical/IBA Reaction Rate Constant

The OH rate constant for isobutyl acetate isobutyl acetate (IBA, $(CH_3)_2CHCH_2OC(=O)CH_3$) was determined using the relative rate method described above. Typically five experimental runs were conducted on each IBA/reference pair. The plot of a modified version of equation (6) is shown in Figure 8. The $\ln([IBA]_0/[IBA]_t)$ term is multiplied by the respective reference rate constant (cyclohexane $(7.49 \pm 1.9) \times 10^{-12}cm^3molecule^{-1}s^{-1}$ and n-nonane $(10.2 \pm 2.6) \times 10^{-12}cm^3molecule^{-1}s^{-1}$) [8] and divided by $10^{-12}cm^3molecule^{-1}s^{-1}$ resulting in a unitless slope that is equal to the hydroxyl radical/IBA rate constant, k_{IBA}, *divided by* $10^{-12}cm^3molecule^{-1}s^{-1}$. This modification allows for a direct comparison to the two reference compound/IBA data sets. The slope of the line yields an hydroxyl radical bimolecular rate constant, k_{IBA}, of $(6.49 \pm 0.07) \times 10^{-12}cm^3molecule^{-1}s^{-1}$. The data points at the origin are experimental points because pre-irradiation, t = 0, data showed no detectable loss of IBA or reference. The error in the rate constant stated above is the 95% confidence level from the random uncertainty in the slope. Incorporating the uncertainties associated with the reference rate constants (± 25%) used to derive the IBA/OH rate constant yields a final value for k_{IBA} of $(6.49 \pm 1.6) \times 10^{-12}cm^3molecule^{-1}s^{-1}$. Assuming an $[OH] = 1 \times 10^6$ molecules cm^{-3}, the atmospheric (1/e) lifetime calculated for IBA is 43 hours. The IBA/OH rate constant, k_{IBA}, has not been previously reported. The observed rate constant is somewhat faster than the k_{IBA} calculated using a structure reactivity relationship, $4.7 \times 10^{-12}cm^3molecule^{-1}s^{-1}$ [9].

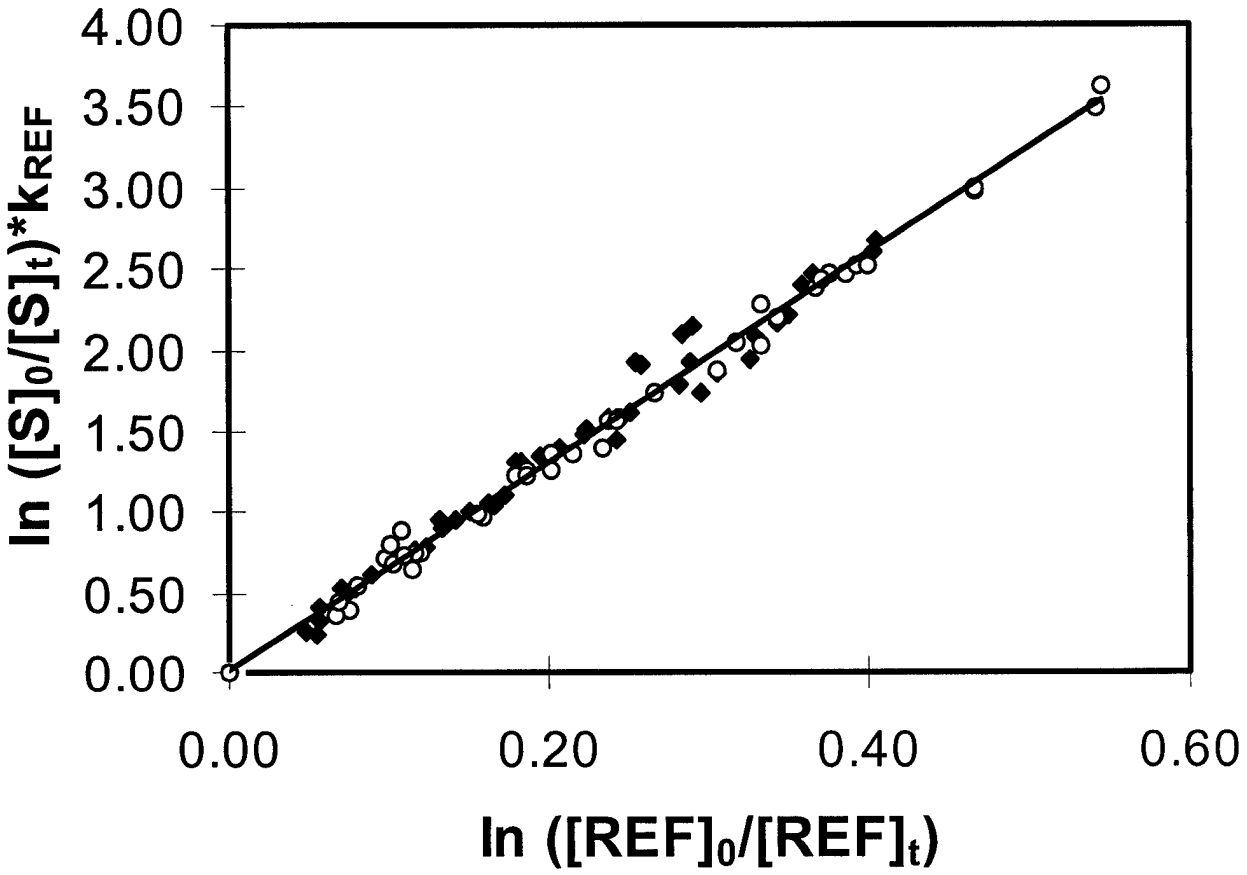

Figure 8. Isobutyl Acetate relative rate plot with both n-nonane (○) and cyclohexane (♦) as reference compounds. The OH + IBA rate constant, k_{IBA}, measured is 6.49 ± 0.07 x 10^{-12} $cm^3 molecule^{-1} s^{-1}$.

6. Hydroxyl Radical/HXA Reaction Rate Constant

The OH rate constant for n-hexyl acetate (HXA, $CH_3(CH_2)_5OC(=O)CH_3$) was determined using the relative rate method described above. Typically five experimental runs were conducted on each HXA/reference pair. The plot of a modified version of equation (6) is shown in Figure 9. The $\ln([HXA]_0/[HXA]_t)$ term is multiplied by the respective reference rate constant (dodecane $(14.2 \pm 3.6) \times 10^{-12}$ $cm^3molecule^{-1}s^{-1}$ and n-nonane $(10.2 \pm 2.6) \times 10^{-12}$ $cm^3molecule^{-1}s^{-1}$) [8] and divided by 10^{-12} $cm^3molecule^{-1}s^{-1}$ resulting in a unitless slope equal to the hydroxyl radical/HXA rate constant, k_{HXA}, *divided by* 10^{-12} $cm^3molecule^{-1}s^{-1}$. This modification allows for a direct comparison to the two reference compound/HXA data sets. The slope of the line yields an hydroxyl radical bimolecular rate constant, k_{HXA}, of $(9.29 \pm 0.16) \times 10^{-12}$ $cm^3molecule^{-1}s^{-1}$. The data points at the origin are experimental points because pre-irradiation, $t = 0$, data showed no detectable loss of HXA or reference. The error in the rate constant stated above is the 95% confidence level from the random uncertainty in the slope. Incorporating the uncertainties associated with the reference rate constants ($\pm$ 25%) used to derive the HXA/OH rate constant yields a final value for k_{HXA} of $(9.3 \pm 2.3) \times 10^{-12}$ $cm^3molecule^{-1}s^{-1}$. Assuming an $[OH] = 1 \times 10^6$ molecules cm^{-3}, the atmospheric (1/e) lifetime calculated for HXA is 30 hours. The HXA/OH rate constant, k_{HXA}, has not been previously reported. The observed rate constant is somewhat faster than k_{HXA} calculated using a structure reactivity, 7.5×10^{-12} $cm^3molecule^{-1}s^{-1}$[9]. The k_{HXA} reported here is in excellent agreement with recently published rate constants for a series of acetates which correlated alkane length with OH reaction rate constant.[18, 19]

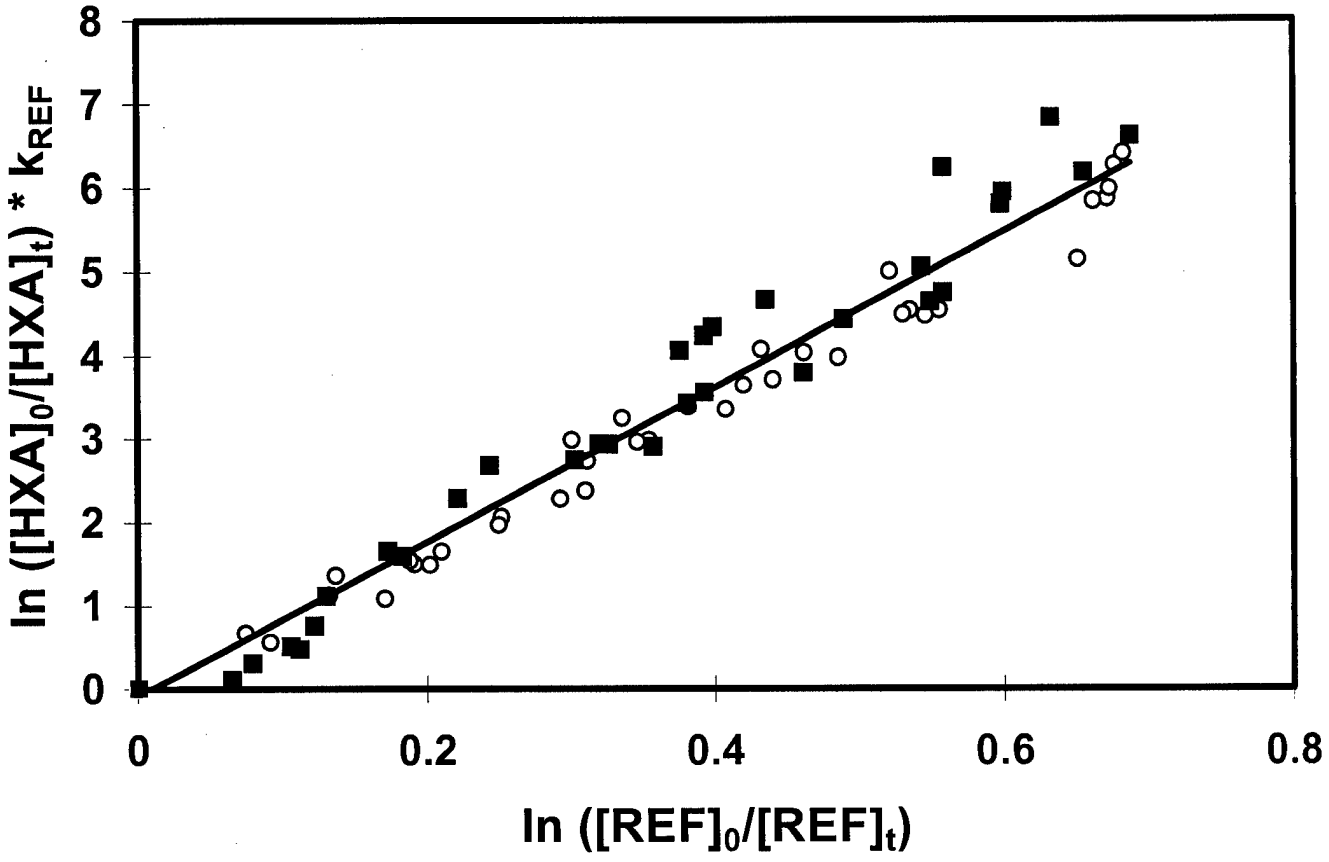

Figure 9. Hexyl Acetate relative rate plot with both n-nonane (O) and dodecane (■) as reference compounds. The OH + HXA rate constant, k_{HXA}, measured is 9.29 ± 0.16 x 10^{-12} $cm^3 molecule^{-1} s^{-1}$.

7. Hydroxyl Radical/MIB Reaction Rate Constant

The OH rate constant for methyl isobutyrate (MIB, $(CH_3)_2$ CHC(=O)-O-CH_3) was obtained using the relative rate method described above. Typically five experimental runs were conducted on each MIB/reference pair. The plot of a modified version of equation (6) is shown in Figure 10. The $\ln([R]_0/[R]_t)$ term is divided by the respective reference rate constant (methyl ethyl ketone (2-butanone) (1.15 ± 0.29) x $10^{-12}$$cm^3molecule^{-1}s^{-1}$, 2,2,4-trimethyl pentane (3.59 ± 0.90) x $10^{-12}$$cm^3molecule^{-1}s^{-1}$and 3-pentanone (2.0 ± 0.5) x $10^{-12}$$cm^3molecule^{-1}s^{-1}$) [8] and multiplied by $10^{-12}cm^3molecule^{-1}s^{-1}$ resulting in a unitless number and yielding a slope that is equal to the hydroxyl radical/MIB rate constant, k_{MIB}, *divided by* $10^{-12}cm^3molecule^{-1}s^{-1}$. This modification allows for a direct comparison of the three reference compound/MIB data sets. The slope of the line yields an hydroxyl radical bimolecular rate constant, k_{MIB}, of (1.73 ± 0.05) x $10^{-12}cm^3molecule^{-1}s^{-1}$. The data points at the origin are experimental points because pre-irradiation, t = 0, data showed no detectable loss of MIB or reference. The error in the rate constant stated above is the 95% confidence level from the random uncertainty in the slope. Incorporating the uncertainties associated with the reference rate constants (± 25%) used to derive the MIB/OH rate constant yields a final value for k_{MIB} of (1.7 ± 0.4) x $10^{-12}cm^3molecule^{-1}s^{-1}$. Assuming an [OH] = 1 x 10^6 molecules cm^{-3}, the atmospheric (1/e) lifetime calculated for MIB is 163 hours. The MIB/OH rate constant, k_{MIB}, has not been previously reported. The observed rate constant can be compared with a k_{MIB} calculated using a structure reactivity relationship [9]. The calculated k_{MIB} was 2 x $10^{-12}cm^3molecule^{-1}s^{-1}$, in agreement with our measured value.

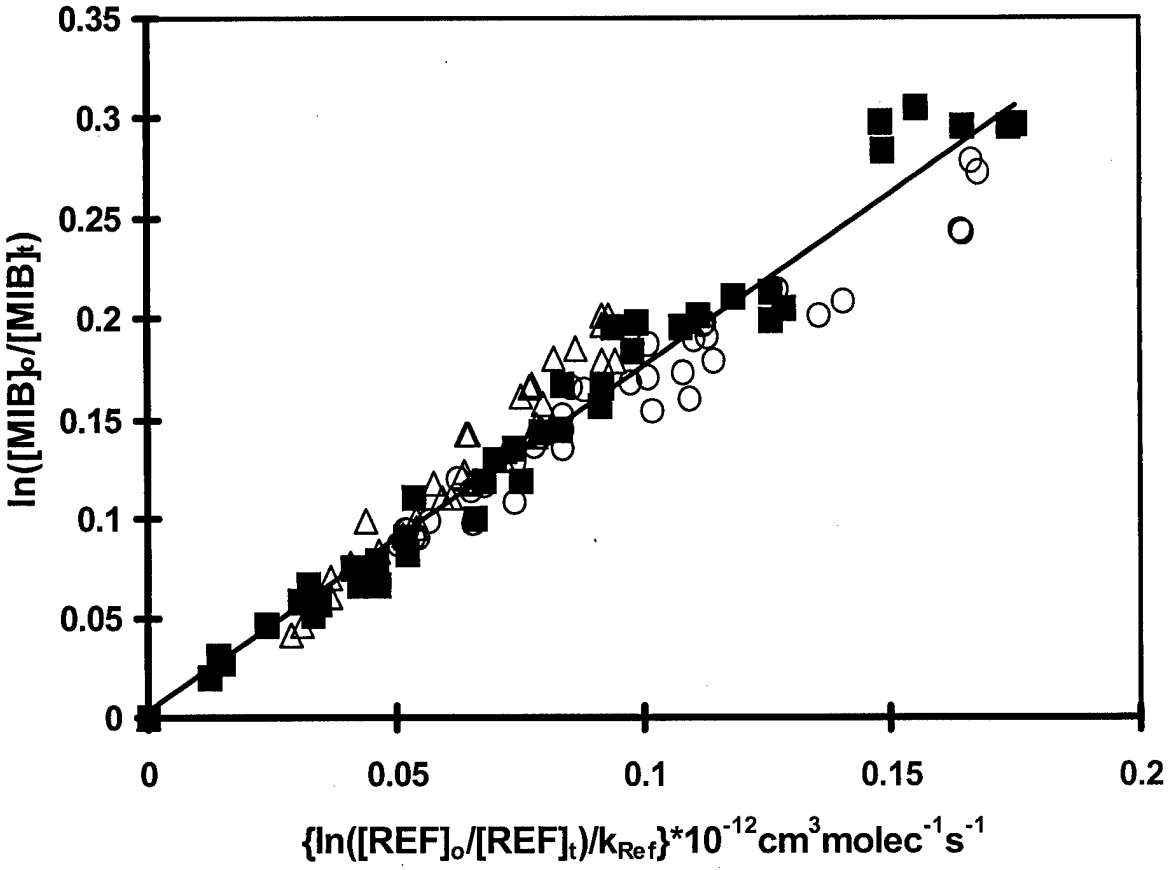

Figure 10. Methyl isobutyrate relative rate plot with methyl ethyl ketone (○), 2,2,4 trimethyl pentane (Δ) and 3-pentanone (■) as reference compounds. The OH + MIB rate constant, k_{MIB}, measured is $1.73 \pm 0.05 \times 10^{-12}$ $cm^3 molecule^{-1} s^{-1}$.

8. Hydroxyl Radical/Siloxane Reaction Rates

The OH rate constants for hexamethyldisiloxane, $(CH_3)_3Si\text{-}O\text{-}Si(CH_3)_3$, octamethyltrisiloxane, $(CH_3)_3Si\text{-}O\text{-}Si(CH_3)_2\text{-}O\text{-}Si(CH_3)_3$, decamethyltetrasiloxane, $(CH_3)_3Si\text{-}O\text{-}Si(CH_3)_2\text{-}O\text{-}Si(CH_3)_2\text{-}O\text{-}Si(CH_3)_3$, were obtained using the relative rate method described above. Typically five experimental runs were conducted on each siloxane/reference pair. The plot of equation (6) with hexane as the reference for all three siloxanes is shown in Figure 11. The MD_2M data set has been offset by 0.05 units on the y axis for clarity. The data points at the origin are experimental points because pre-irradiation, t = 0, data showed no detectable loss of siloxane or reference. The slopes of these linear plots in Figure 11 are multiplied by the OH rate constant for hexane (5.61 x 10^{-12} $cm^3molecule^{-1}s^{-1}$ [8]) yielding the rate constant for the respective siloxane. Similar rate constant plots were constructed for cyclohexane ((reference for MM and MD_2M) 7.49 x 10^{-12} $cm^3molecule^{-1}s^{-1}$[8]) and n-nonane ((reference for MDM) 10.2 x 10^{-12} $cm^3molecule^{-1}s^{-1}$[8]) as reference compounds. The siloxane/reference plots resulted in MM + OH, MDM + OH , and MD_2M + OH having bimolecular rate constants of 1.32 ± 0.05 x 10^{-12} $cm^3molecule^{-1}s^{-1}$, 1.83 ± 0.09 x 10^{-12} $cm^3molecule^{-1}s^{-1}$, 2.66 ± 0.13 x 10^{-12} $cm^3molecule^{-1}s^{-1}$, respectively. The errors in the rate constants are the 95% confidence level from the random uncertainty in the slope. This error does not include uncertainties associated with the reference rate constant that was used to derive the siloxane/OH rate constant. The MM/OH rate constant has been measured previously by Atkinson *et al.* (1.38 ± 0.36 x 10^{-12} $cm^3molecule^{-1}s^{-1}$ [20]) and Sommerlade *et al.* (1.19 ± 0.30 x 10^{-12} $cm^3molecule^{-1}s^{-1}$ [21]), and our MM/OH measurement is in agreement with the literature. To the best of our knowledge, the OH rate constants for MDM and MD_2M have not been

previously reported. Assuming an [OH] = 1 x 10^6 molecules cm^{-3}, the atmospheric (1/e) lifetimes calculated for MM, MDM, MD_2M are 8.8, 6.3, and 4.3 days, respectively.

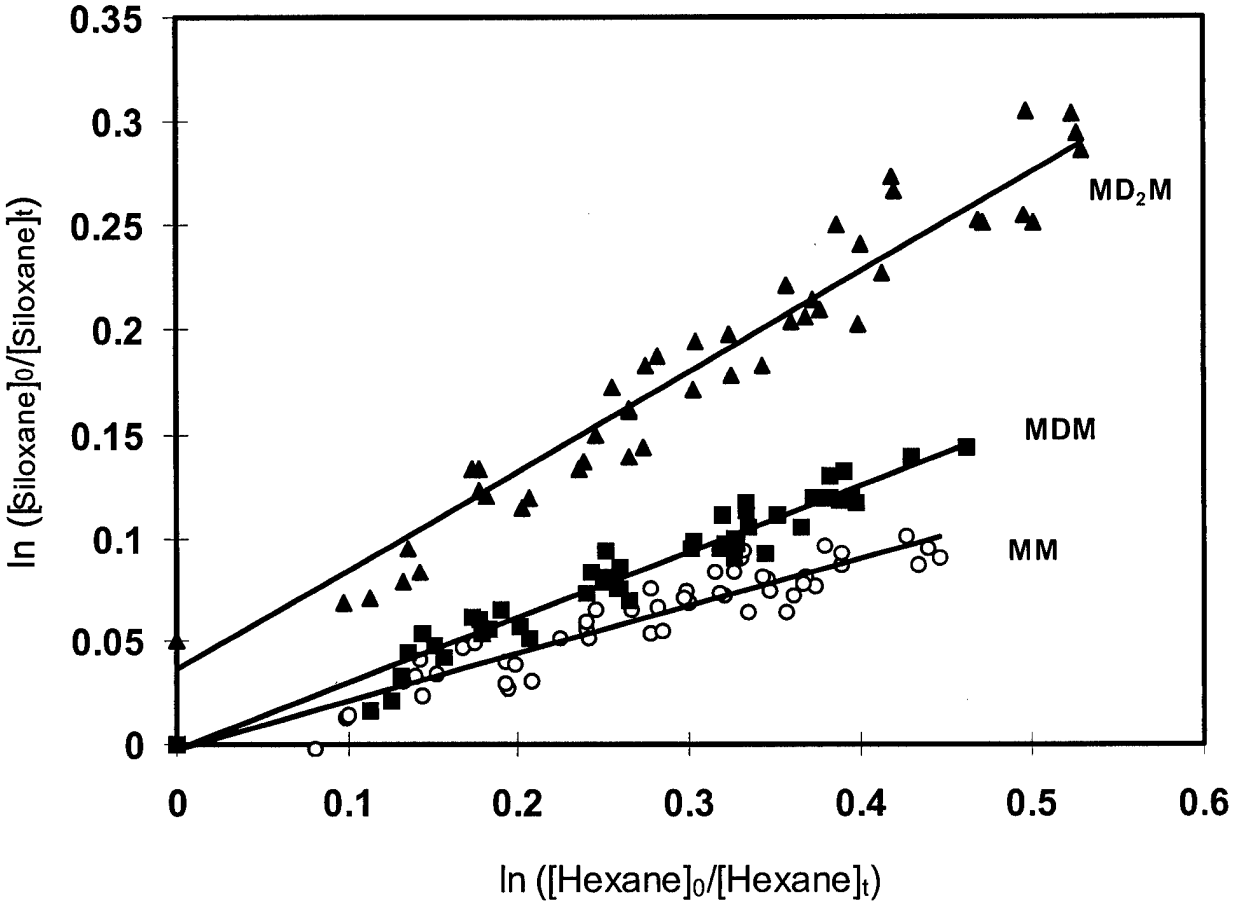

Figure 11. Plot of the relative rate of siloxane/OH reaction for hexamethyldisiloxane (MM,○, $(CH_3)_3Si\text{-}O\text{-}Si(CH_3)_3$), octamethyltrisiloxane (MDM,■, $(CH_3)_3Si\text{-}O\text{-}Si(CH_3)_2\text{-}O\text{-}Si(CH_3)_3$), decamethyltetrasiloxane (MD_2M, ▲,$(CH_3)_3Si\text{-}O\text{-}Si(CH_3)_2\text{-}O\text{-}Si\ (CH_3)_2\text{-}O\text{-}Si(CH_3)_3$) against the reference compound, *n*-hexane. MD_2M data is shifted *up* on the y axis by 0.05 units to avoid confusion with MM and MDM. The slopes of the linear least squares analysis with 95% confidence intervals are 0.231 ± 0.008, 0.320 ± 0.016, 0.4807 ± 0.023 for MM, MDM, and MD_2M, respectively.

Table 1. Hydroxyl radical rate constants and chemical structure of volatile organic compounds investigated

Compound	Structure	OH rate constant ($*10^{12}cm^{-3}$molecule s)
Ethyl 3-ethoxypropionate	$CH_3CH_2OCH_2CH_2C(=O)OCH_2CH_3$	22.9 ± 7.4
2-Ethoxyethanol	$CH_3CH_2OCH_2CH_2OH$	15.8 ± 3.8
2-Butoxyethanol	$CH_3CH_2CH_2CH_2OCH_2CH_2OH$	22.5 ± 5.6
2-Propoxyethanol	$CH_3CH_2CH_2OCH_2CH_2OH$	21.4 ± 6.0
2-Butanol	$CH_3CH(OH)CH_2CH_3$	8.1 ± 2.0
2-Pentanol	$CH_3CH(OH)CH_2CH_2CH_3$	11.9 ± 3.0
Isobutylacetate	$(CH_3)_2CHCH_2OC(=O)CH_3$	6.5 ± 1.6
Hexylacetate	$CH_3(CH_2)_5OC(=O)CH_3$	9.3 ± 2.3
Methyl isobutyrate	$(CH_3)_2CHC(=O)$-O-CH_3	1.7 ± 0.4
Hexamethyldisiloxane	$(CH_3)_3Si$-O-$Si(CH_3)_3$	1.32 ± 0.05
Octamethyltrisiloxane	$(CH_3)_3Si$-O-$Si(CH_3)_2$-O-$Si(CH_3)_3$	1.83 ± 0.09
Decamethyltetrasilozane	$(CH_3)_3Si$-O-$Si(CH_3)_2$-O-$Si(CH_3)_2$-O-$Si(CH_3)_3$	2.66 ± 0.13

B. REACTION PRODUCT STUDIES

Identification and quantification of OH/VOC reaction products yields valuable insights for assessment of the VOC's impact on air quality. VOC atmospheric transformation mechanisms when coupled with pertinent rate constants are important for assessing VOC incremental reactivity (tendency to generate ground level ozone). Reaction product investigations are also important for preventing release of toxic chemical precursors. The parent VOC might have low or no toxicity, but the daughter products could be toxic. Depending on the yield and intermediate reaction rate constants, reaction product toxicity could be an important factor in compound selection. Below are the reaction products observed for the VOC's investigated.

Because the OH/VOC reaction products could react with OH, the observed product concentrations had to be corrected for OH + reaction product reactions. This correction has been described in detail [22, 23] and has the following form:

(8) $$F = \frac{(k_{VOC} - k_P)}{k_{VOC}} \times \frac{1 - \frac{[VOC]_t}{[VOC]_0}}{\left(\frac{[VOC]_t}{[VOC]_0}\right)^{k_P/k_{VOC}} - \frac{[VOC]_t}{[VOC]_0}}$$

F, the correction factor, was multiplied by the product concentration data; k_{EEP} is the OH + VOC rate constant, and k_P is the rate constant for the reaction of OH with reaction product. The measured value for k_P was used when possible, but k_P was calculated using structure reactivity [6] when no measured value was available in the literature. It should be noted that all of the products exhibited linear concentration profiles; the lack of curvature strongly suggesting no unusual side reactions that generate or remove primary reaction products. For completeness, the k_P values are presented with the respective product.

1. OH/EEP Reaction Products

The reaction products observed are in accordance with previously observed hydroxyl radical reaction mechanisms for oxygenated organic species [22, 24-26]. Typically, the oxygenated organic parent compound reacts with OH to subsequently generate other oxygenated organic products. For EEP, the OH/EEP reaction products observed were: ethyl glyoxate (EG, HC(=O)C(=O)-O-CH_2CH_3), ethyl (2-formyl) acetate (EFA, HC(=O)-CH_2-C(=O)-O-CH_2CH_3), ethyl (3-formyloxy) propionate (EFP, HC(=O)-O-CH_2CH_2-C(=O)-O-CH_2CH_3), ethyl formate (EF, HC(=O)O-CH_2CH_3), acetaldehyde (HC(=O)CH_3), diethyl malonate (DM, CH_3-CH_2-O-C(=O)-CH_2-C(=O)O-CH_2CH_3). The specific results for each of these products are described below. The reported yields are based on the slopes of the EEP reacted versus product formed plots. The reported error in

the product yield is the 95% confidence level from the random uncertainty in the slope of these plots.

a. Ethyl (3-formyloxy) propionate (EFP, HC(=O)-O-CH_2CH_2-C(=O)-O-CH_2CH_3)

EFP is the reaction product retaining most of the parent EEP molecule. Its assignment was based on analysis of both the FTIR and mass spectrum of the chromatographic peak. This product was not commercially available and an unequivocal verification was not possible. The assignment of this product is reasonable, however, due to the recently published observation of ethanediol acetate formate (EAF, CH_3-C(=O)O-CH_2CH_2-O-C(=O)H) as an OH/2-ethoxyethyl acetate (EEA, CH_3-C(=O)O-CH_2CH_2-O-CH_2CH_3) reaction product [24]. Using the same separation parameters, EFP and EAF behave similarly chromatographically having a retention time later than the parent compound. In fact, the calibration of EFP was extracted from the calibration of EAF by correcting for the additional carbons in the EFP molecule. The GC/FID system was used to monitor EFP concentrations. The k_{EFP} calculated using structure reactivity [9] was 8.34 x 10^{-12} $cm^3molecule^{-1}s^{-1}$. From equation 8 the average [EFP] correction was 13.3% (maximum correction 31%). The yield of EFP was 30 ± 1 %.

b. Ethyl formate (EF, HC(=O)O-CH_2CH_3)

Ethyl formate was identified by GC/FTIR/MS and quantitated by GC/FID. Pure EF was obtained to verify product assignment. A 37 ± 1 % EF yield from OH + EEP reaction was observed. The rate constant for OH + EF (1.02 x $10^{-12}cm^3molecule^{-1}s^{-1}$) measured by Wallington *et al.* [27] was used for k_P in equation 8 and resulted in an average [EF] correction of 1.5% (maximum correction 2.6%).

c. Ethyl (2-formyl) acetate (EFA, HC(=O)-CH_2-C(=O)-O-CH_2CH_3)

EFA was derivatized using DNPH, identified using LC/MS and quantitated using LC. EFA was not commercially available, however hydrazone concentration calibrations are quite similar compound to compound, because the absorption signal comes mainly from the dinitrophenyl rings on the DNPH and are not especially sensitive to hydrocarbon type. k_{EFA} was calculated [9] (2.18×10^{-12} $cm^3molecule^{-1}s^{-1}$), and the average [EFA] correction was on the order of 3% (maximum correction 4.6%). The observed EFA yield was 4.8 ± 0.2 %.

d. Ethyl glyoxate (EG, $HC(=O)C(=O)\text{-}O\text{-}CH_2CH_3$)

EG was derivatized using DNPH, identified using LC/MS and quantitated using LC. EG is commercially available as a 50/50 mixture with toluene. The [EG] analysis was slightly more complicated due to the splitting of the EG signal into two chromatographic peaks. This observation indicates there may be two forms of the derivatized hydrazone. For equation 8, k_{EG} was calculated [9] to be 1.66×10^{-12} $cm^3molecule^{-1}s^{-1}$. The EG yield was 25 ± 1 % with an average [EG] correction of 2.2% (maximum correction 4.5%).

e. Acetaldehyde ($HC(=O)CH_3$)

Acetaldehyde was derivatized using DNPH and identified and quantitated by LC. Acetaldehyde was commercially available and used for calibrations and assignment verification. $k_{Acetaldehyde}$ is reported in the literature (1.5×10^{-11} $cm^3molecule^{-1}s^{-1}$) [28-30]. The acetaldehyde yield was 4.9 ± 0.2 % with an average [acetaldehyde] correction of 22% (maximum correction 47%). This large correction was due mainly to the fast reaction of acetaldehyde with OH.

f. Diethyl Malonate (DM, $CH_3\text{-}CH_2\text{-}O\text{-}C(=O)\text{-}CH_2\text{-}C(=O)O\text{-}CH_2CH_3$)

While not quantitated due to a very small yield, DM, observed by GC/MS/FTIR, is included for completeness. Both the mass and infrared spectra observed matched the respective spectral libraries. This combined with the structural similarity to EEP made the assignment very conclusive.

The following table is a summation of the above results:

Table 2. OH/EEP Reaction Products and Yields

Reaction Product	Structure	Yield (Corrected for reaction with OH)
Ethyl (3-formyloxy)propionate	$HC(=O)\text{-}O\text{-}CH_2CH_2C(=O)OCH_2CH_3$	30 ± 1%
Ethyl Formate	$HC(=O)O\text{-}CH_2CH_3$	37 ± 1%
Ethyl Glyoxate	$HC(=O)C(=O)\text{-}O\text{-}CH_2CH_3$	25 ± 1%
Ethyl (2-formyl) acetate	$HC(=O)CH_2\text{-}C(=O)O\text{-}CH_2CH_3$	4.8 ± 0.2%
Acetaldehyde	$HC(=O)CH_3$	4.9 ± 0.2%

2. OH/Hydroxy ethers Reaction Products

The 2EEOH/OH and 2BEOH/OH reaction products observed are consistent with previously observed hydroxyl radical reaction mechanisms for oxygenated organic species [11, 14, 22, 24-26, 32, 33]. Typically, the oxygenated organic parent compound reacts with OH to subsequently generate other oxygenated organic products. For 2EEOH and 2BEOH, the major OH/hydroxy ether reaction products observed were aldehydes and formates. The specific product results for each hydroxy ether are described in separate sections below. The reported yields are based on the slopes of the hydroxy ether reacted versus product formed plots. The reported error in the product yield is the 95% confidence level from the random uncertainty in the slope of these plots.

a. 2-Ethoxyethanol/OH Reaction Product Results

Three products were observed from the 2-ethoxyethanol/OH reaction: ethyl formate (EF, detected via GC/FTIR/MS and quantified by GC/FID), 2-methyl-1,3-

dioxolane (detected by GC/FTIR/MS) and acetaldehyde (detected and quantified by DNPH derivatization). The product results data are summarized in Table 3 below.

Table 3. 2-Ethoxyethanol/OH Reaction Product Data and Correction Factors

Product	Structure	Yield %	$k_{Product}$ (units of 10^{-12} molecule^{-1}s^{-1})	F_{avg} %	$F_{Maximum}$ %
Ethyl formate	$CH_3CH_2OC(=O)H$	37 ± 4	1.15 [8]	1.6	3.5
Acetaldehyde	$HC(=O)CH_3$	5 ± 1	15.8 [8, 28-30]	27	62
2-Methyl-1,3-dioxolane	Cyclic ether	Detected			

$k_{Product}$ is the OH/product reaction bimolecular rate constant, F_{avg} is the average correction factor calculated using equation 8 for the yield data set, and $F_{Maximum}$ is the largest correction factor calculated using equation 8 for the yield data set

The large correction for acetaldehyde was due mainly to the large value of $k_{Acetaldehyde}$ relative to k_{2EEOH}.

Three peaks remained unidentified in the DNPH derivatization chromatograms. Typically, the chromatographic calibration factors are similar for the hydrazones and the unidentified peaks had areas correlating to very small product percentage yields. The only reaction product identified in reference 11 that would be DNPH active was ethoxyacetaldehyde ($CH_3CH_2OCH_2C(=O)H$). However its yield of 24% reported in reference 11 would have been a significant peak in our DNPH experimental runs.

b. 2-Butoxyethanol/OH Reaction Product Results

Five products were observed from the 2-butoxyethanol/OH reaction: butyl formate (BF, detected by GC/FTIR/MS and quantified by GC/FID), propionaldehyde (detected and quantified by DNPH derivatization), acetaldehyde (detected and quantified by DNPH derivatization), and 2-propyl-1,3-dioxolane (detected via GC/FTIR/MS). The product results data are summarized in Table 4 below.

Table 4. 2-Butoxyethanol/OH Reaction Product Data and Correction Factors

Product	Structure	Yield %	$k_{Product}$ (units of 10^{-12} molecule^{-1}s^{-1})	F_{abg} %	$F_{Maximum}$ %
Butyl formate	$HC(=O)OCH_2CH_2CH_2CH_3$	30 ± 2	3.12 [27]	4.5	9.6
Propionaldehyde	$HC(=O)CH_2CH_3$	13 ± 1	19.6 [8]	53	126
Acetaldehyde	$HC(=O)CH_3$	3.7 ± 0. 4	15.8 [8, 28-30]	24	53
Butyraldehyde	$HC(=O)CH_2CH_2CH_3$	2.8 ± 0.2	19.6 [34]	42	98
2-Propyl-1,3-dioxolane	Cyclic ether	detected			

$k_{Product}$ is the OH/product reaction bimolecular rate constant, F_{avg} is the average correction factor calculated using equation 8 for the yield data set, and $F_{Maximum}$ is the largest correction factor calculated using equation 8 for the yield data set

The large correction for propionaldehyde yield was due mainly to the large value of $k_{Propionaldehyde}$ relative to k_{2BEOH}.

Two peaks remained unidentified in the DNPH chromatograms. The calibration factors for the hydrazones were all quite similar and the unidentified peaks had areas correlating to very small percentage yields. The only reaction products identified in reference 14 that would be DNPH active were butoxyacetaldehyde ($CH_3(CH_2)_3OCH_2C(=O)H$).

3. OH/2-Propoxyethanol Reaction Products

The 2PEOH/OH reaction products observed are consistent with previously observed hydroxyl radical reaction mechanisms for oxygenated organic species [11, 14, 22, 24-26, 32, 33, 35]. Typically, the oxygenated organic parent compound reacts with OH to subsequently generate other oxygenated organic products. For 2PEOH, the major reaction product observed was propyl formate. The specific reaction product results are described in a separate section below. The reported yields are based on the slopes of the

2PEOH reacted versus product formed plots. The reported error in the product yield is the 95% confidence level from the random uncertainty in the slope of these plots.

Three products were observed from the 2-propoxyethanol/OH reaction: propyl formate (PF, detected via GC/MS and quantified by GC/FID), 2-propyl-1,3-dioxolane (detected by GC/MS and quantified by GC/FID) and 2-propoxyethanal (detected by GC/MS and quantified by GC/FID). The product results data are summarized in Table 5 below.

Table 5. 2-Propoxyethanol/OH Reaction Product Data and Correction Factors

Product	Structure	Yield %	$k_{Product}$ (units of 10^{-12} molecule^{-1}s^{-1})	F_{avg} %	$F_{Maximum}$ %
Propyl formate	$CH_3CH_2CH_2OC(=O)H$	47 ± 2	2.38 [27]	1.9	4.5
Propoxyethanal	$CH_3CH_2CH_2OCH_2CH(=O)$	15 ± 1	26.8 [9]	24	60
2-Ethyl-1,3-dioxolane	Cyclic ether	5.4 ±0.4	26.2 [9]	23	59

$k_{Product}$ is the OH/product reaction bimolecular rate constant, F_{avg} is the average correction factor calculated using equation 8 for the yield data set, and $F_{Maximum}$ is the largest correction factor calculated using equation 8 for the yield data set

One other reaction product was observed in the product experiments, however a plot of its formation versus 2PEOH loss was curved and inconsistent. This could indicate this product was either a secondary reaction product (i.e. reaction product of reaction products), reacted with some other species, or was formed from wall reactions. Interpretation of the mass spectra indicates that this product is likely to be another oxygenated organic compound such as $CH_3C(=O)CH_2OCH_2CH_2OH$.

Only formaldehyde was observed in DNPH derivatization experiments, however formaldehyde is a product of methyl nitrite photolysis. Its quantitation requires use of a different hydroxyl radical source.

4. OH/Secondary Alcohols Reaction Products

The observed OH/alcohol reaction products are consistent with previously observed hydroxyl radical atmospheric chemistry reaction mechanisms for organic compounds [22, 24-26]. For 2BU and 2PE, the major OH/alcohol reaction products observed were ketones of the same length as the alcohol and the carbonyl group in the same position as the hydroxyl group of the parent alcohol. The specific product results for each alcohol are described in separate sections below. The reported yields are based on the slopes of the alcohol reacted versus product formed plots. The reported error in the product yield is the 95% confidence level from the random uncertainty in the slope of these plots.

a. 2-Butanol/OH Reaction Product Results

Two major products were observed from the 2-butanol/OH reaction: methyl ethyl ketone (MEK) and acetaldehyde. Quantification of MEK yields was achieved with GC/FID and DNPH derivatization was used to quantify acetaldehyde yields. The product results data are summarized in Table 6.

The large correction for acetaldehyde was due mainly to the large value of $k_{Acetaldehyde}$ relative to k_{2BU}.

b. 2-Pentanol/OH Reaction Product Results

Three major products were observed from the 2-pentanol/OH reaction: 2-pentanone, propionaldehyde, and acetaldehyde. Quantification of both 2-pentanone and propionaldehyde yields was achieved with GC/FID and DNPH derivatization was used to quantify acetaldehyde yields. The product results data are summarized in Table 6.

The large corrections for propionaldehyde and acetaldehyde were due mainly to the large value of $k_{Product}$ relative to k_{2PE}.

Table 6. 2-Butanol/OH and 2-Pentanol/OH Reaction Product Data and Correction Factors

Product	Structure	Yield %	$k_{Product}$ (units of 10^{-12} molecule^{-1}s^{-1})	F_{avg} %	$F_{Maximum}$ %
2-BUTANOL					
Methyl Ethyl Ketone	$CH_3C(=O)CH_2CH_3$	60 ± 2	1.15 [8]	1.8	3.6
Acetaldehyde	$HC(=O)CH_3$	29 ± 4	15.8 [8, 28-30]	41	127
2-PENTANOL					
2-Pentanone	$CH_3C(=O)(CH_2)_2CH_3$	41 ± 4	4.9 [8]	7	12
Propionaldehyde	$HC(=O)CH_2CH_3$	14 ± 2	19.6 [8]	30	86
Acetaldehyde	$HC(=O)CH_3$	40 ± 4	15.8 [8, 28-30]	24	67

$k_{Product}$ is the OH/product reaction bimolecular rate constant, F_{avg} is the average correction factor calculated using equation 8 for the yield data set, and $F_{Maximum}$ is the largest correction factor calculated using equation 8 for the yield data set

5. OH/Acetates Reaction Products

a. OH/IBA Reaction Products

The reaction products observed follow trends previously observed hydroxyl radical reaction mechanisms for oxygenated organic species [22, 24-26]. Typically, the oxygenated organic parent compound reacts with OH to subsequently generate other oxygenated organic products. For IBA, the OH/IBA reaction products observed were acetone ($(CH_3)_2C=O$) and acetic acid ($HOC(=O)CH_3$). The specific results for each of these products are described below. The reported yields are based on the slopes of the IBA reacted versus product formed plots. The reported error in the product yield is the 95% confidence level from the random uncertainty in the slope of these plots.

The two main IBA/OH reaction products observed were acetone ($(CH_3)_2C(=O)$) and acetic acid ($HOC(=O)CH_3$). Acetone was identified and quantitated by GC/MS. Pure acetone was obtained to verify product assignment. A 62 ± 2.9% yield from OH + IBA reaction was observed. The rate constant for OH + Acetone (0. 219 x 10^{-12} $cm^3molecule^{-1}s^{-1}$) was used for k_P in equation 8 and resulted in an average [acetone] correction of 0.3% (maximum correction of 1.1%).[8]

Acetic acid yield results were inconclusive. Changes in the acetic acid concentration during the course of the reaction resulted in chromatographic changes (e.g., change in peak shaped, retention time) that made quantitation exceedingly difficult. Acetic acid was identified by GC/FID/MS and GC/MS/FTIR. Pure acetic acid was obtained to verify product assignment and confirm observed mass spectrum.

Results of DNPH derivatizations yielded no new observed products.

b. OH/HXA Reaction Products

Several OH/HXA reaction products were observed and tentatively identified, but they were in such low yields that quantitation was not possible. This result is probably due to the several possible hydrogen abstraction sites on the HXA molecule. Even if the several product were quantitated their yields would probably not add up significantly to account for the amount of HXA lost due to reaction with OH. This suggests possible particulate processes and/or chemical pathways that result in undetectable products. However, the observed products do highlight unusual ring closure mechanisms that do not involve oxidation of NO to NO_2. The proposed OH/HXA reaction products inferred from mass spectrum data were: acetic acid, two ringed compounds (proposed to be β-butyl-γ-butyrolactone and α-methylpropyl-γ-butyrolactone), an unidentified nitrate,

$HC(=O)CH_2CH_2CH_2O(O=)CCH_3$, 5-hexanone acetate ($CH_3C(=O)CH_2CH_2CH_2CH_2OC(=O)CH_3$), 4-hexanone acetate ($CH_3CH_2C(=O)CH_2CH_2CH_2OC(=O)CH_3$) and hexanal ($HC(=O)CH_2CH_2CH_2CH_2CH_3$).

6. OH/MIB Reaction Products

The reaction products observed are in accordance with previously observed hydroxyl radical reaction mechanisms for oxygenated organic species [22, 24-26]. Typically, the oxygenated organic parent compound reacts with OH to subsequently generate other oxygenated organic products. For MIB, the OH/MIB reaction products observed were: acetone and methyl pyruvate. The specific results for each of these products are described below. The reported yields are based on the slopes of the MIB reacted versus product formed plots. The reported error in the product yield is the 95% confidence level from the random uncertainty in the slope of these plots.

a. Acetone ($(CH_3)_2C(=O)$)

The GC/MS/FTIR system was used to monitor acetone concentrations. The $k_{Acetone}$ has been measured [8] and a value of 0.219×10^{-12} $cm^3molecule^{-1}s^{-1}$ was used in equation 8. From equation 8 the average [Acetone] correction was 1.5% (maximum correction 4.2%). The yield of acetone was 97 ± 1 %.

b. Methyl pyruvate (MP, $CH_3C(=O)C(=O)$-O-CH_3)

Methyl pyruvate was identified and quantified by GC/FTIR/MS. Pure MP was obtained to verify product assignment. A 3.3 ± 0.3 % MP yield from OH + MIB reaction was observed. The rate constant for OH + MP, $0.318 \times 10^{-12} cm^3molecule^{-1}s^{-1}$, calculated using structure reactivity [9], was used for k_P in equation 8 and resulted in an average [MP] correction of 2.1% (maximum correction 5.3%).

The following table is a summation of the above results:

Table 7. OH/Methyl isobutyrate Reaction Product Yields

Reaction Product	Structure	Yield (Corrected for reaction with OH)
Acetone	$(CH_3)_2C=O$	97 ± 1%
Methyl pyruvate	$CH_3C(=O)C(=O)OCH_3$	3.3 ± 0.3 %

7. Hydroxyl Radical/Siloxane Reaction Products

OH/siloxane reaction products were observed in experiments performed in a similar manner to the reaction rate experiments except the reference compound was excluded from the reaction mixture. For clarification the observed products will be grouped by parent siloxane.

a. Hexamethyldisiloxane (MM)

The two main products observed in the OH/MM reaction were trimethylsilanol ($(CH_3)_3Si$-OH) and pentamethyldisiloxanol (MDOH, $(CH_3)_3Si$-O-$Si(CH_3)_2$OH). MDOH has been observed as an MM/OH reaction product by Carter *et al.*[36]. Atkinson *et al.* [37] have recently reported that MDOH is most likely a "secondary" product with the primary ester ($(CH_3)_3Si$-O-$(CH_3)_2Si$-OCHO) reacting with water to form MDOH. Because of the humidity of the air surrounding our experimental chambers, this could explain the observation of the silanol formation.

The calibration factor used to determine the concentration of MDOH was the average of the calibration factors for MM, MDM, and MD_2M. The calibration factors for the three siloxanes were almost identical leading to the reasonable assumption that the addition of an OH group onto the siloxane backbone would have a negligible effect on the calibration factor.

The same calibration assumptions made for MDOH cannot be made for $(CH_3)_3SiOH$, because the -OH group may have an effect on the calibration factor versus $(CH_3)_4Si$. In any event, the $(CH_3)_3SiOH$ yield data were not linear and therefore not conclusive.

b. Octamethyltrisiloxane (MDM)

The MDM/OH reaction products observed included 1,1,3,3,5,5,5-heptamethyl-1-trisiloxanol (MD_2OH, $(CH_3)_2Si(OH)\text{-}O\text{-}(CH_3)_2Si\text{-}O\text{-}Si(CH_3)_3$), 1,1,1,3,5,5,5-heptamethyl-3-trisiloxanol (M_2TOH, $(CH_3)_3Si\text{-}O\text{-}(CH_3)Si(OH)\text{-}O\text{-}Si(CH_3)_3$), $(CH_3)_3SiOH$, MDOH, hexamethylcyclotrisiloxane (D_3, $((CH_3)_2Si\text{-}O)_3$), octamethylcyclotetrasiloxane, (D_4, $((CH_3)_2Si\text{-}O)_4$). The major products observed were MD_2OH and M_2TOH. The rational for the calibrations of these compounds is the same as above for MDOH. The determination of calibration factors for these siloxanols was calculated in the same manner as MDOH above. The observed gap in product formation may be an indication that these siloxanols are indeed secondary products resulting from the ester, OCHO-Si -R_1R_2 [37], reacting with water. No siloxane ester was observed using the experimental system described. The gap in the plot could be because a) the k_{H2O} rate constant is slow, b) a low concentration of OCHO-Si -R_1R_2 or c) a combination of both. The formation of the observed siloxanols might indeed be a complicated process.

Both $((CH_3)_2Si\text{-}O)_3$ and $((CH_3)_2Si\text{-}O)_4$ were verified on the GC/FID system by comparing the retention times of the pure cyclic siloxanes versus the observed experimental product retention times. $((CH_3)_2Si\text{-}O)_3$ was also verified by comparing the mass spectrum of the product versus the mass spectrum of the pure compound. The $((CH_3)_2Si\text{-}O)_4$ product has one more dimethylsilicone moiety than the parent compound.

This is unusual and suggests that potential heterogeneous wall reactions may be occurring. Both of the cyclic siloxane products observed were commercially available so that calibration factors could be determined and the observed yield for each cyclic compound was on the order of 4%.

c. Decamethyltetrasiloxane (MD_2M)

All of the observed products for MD_2M/OH were in low and inconsistent concentrations resulting in nonlinear [product] versus [MD_2M] yield plots, suggesting a significant product loss mechanism. Sticking to the chamber walls could be the main reason for the nonlinear yield data and lack of a major product(s). However, some products were observed: MD_2OH, M_2TOH, $(CH_3)_3SiOH$, MDOH, $((CH_3)_2Si\text{-}O)_4$ and other unidentified products. As the reaction products get bigger, there could be a sticking process that would prevent the compounds from being observed.

Some unusual OH + siloxane reaction products were observed and verified. The cyclic siloxane products formed were unusual and unexpected.

SECTION IV

DISCUSSION

A. OH RATE CONSTANTS OF COMPOUNDS INVESTIGATED

All of the VOC's investigated reacted with the OH radical via H-atom abstraction. A wide range of rate constants was observed (see Table 1). The OH rate constants observed were consistent with structural reactivity calculations suggesting that molecular structure is an important factor in OH/VOC kinetic processes. It was observed that the methylenes adjacent to an ether oxygen were very reactive sites.

B. TRANSFORMATION MECHANISMS OF COMPOUNDS INVESTIGATED

1. EEP Transformation Mechanism

OH reacts with EEP by H-atom abstraction. EEP is a large molecule with *six* possible carbons as hydrogen abstraction sites. However, the products of the reaction of OH with EEP suggest strongly that the OH abstracts hydrogen principally from *three* methylene groups. The "reactive structure" of EEP can be drawn as shown in Structure 1:

$$\underset{}{CH_3 - \underset{I}{\underline{C}H_2} - O - \underset{II}{\underline{C}H_2} - \underset{III}{\underline{C}H_2} - \mathbf{R}}$$

Structure 1

where **R** = -C(=O)O-CH_2CH_3. This is consistent with the reaction mechanisms proposed for methylenes attached to an ether oxygen [24,25], and consistent as the sites having the largest contribution to the calculated k_{EEP} using structure reactivity [9]. Also, the agreement between the calculated versus the measured k_{EEP} supports these "reactive site" assignments.

The experimental parameters were set to minimize other side reactions and highlight the first OH hydrogen abstraction step. Nitric oxide (NO) was added to facilitate the generation of OH and to minimize ozone (O_3) and NO_3 formation preventing other possible radical reactions. The proposed OH reaction mechanism is shown in Figure 12.

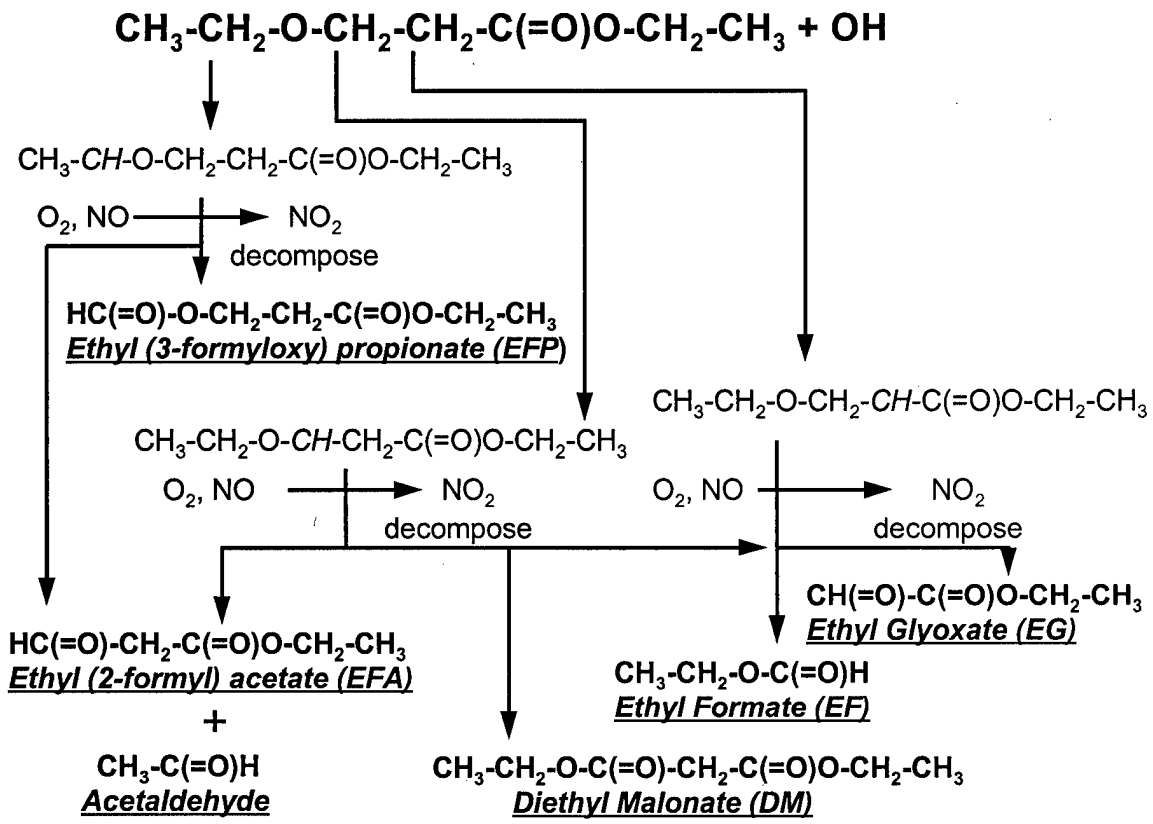

Figure 12. Proposed reaction mechanism for hydroxyl radical with ethyl 3-ethoxypropionate. Major products are in bold typeface.

Depending on the nature of the radical formed in Reaction (4):

For methylene I:

CH_3-C$\underline{H}_2$-O-CH_2-CH_2-**R** + OH → CH_3-(C$\underline{H}$•)-O-CH_2-CH_2-**R** + H_2O (9)

CH_3-(C$\underline{H}$•)-O-CH_2-CH_2-**R** + O_2 + NO → CH_3-(C$\underline{H}$O•)-O-CH_2-CH_2-**R** + NO_2 (10a)

CH_3-(C$\underline{H}$O•)-O-CH_2-CH_2-**R** → H(O=)C-O-CH_2-CH_2-**R** (**EFP**) + •CH_3 (10b)

CH_3-(C$\underline{H}$O•)-O-CH_2-CH_2-**R** + O_2 → CH_3-C(=O)H (**Acetaldehyde**) + H(O=)C-CH_2-**R** (**EFA**) + HO_2 (10c)

For methylene II:

CH_3-CH_2-O-C$\underline{H}_2$-CH_2-**R** + OH → CH_3-CH_2-O-(C$\underline{H}$•)-CH_2-**R** + H_2O (11)

CH_3-CH_2-O-(C$\underline{H}$•)-CH_2-**R** + O_2 + NO → NO_2 + CH_3-CH_2-O + H(O=)C-CH_2-**R**(**EFA**) (12a)

CH_3-CH_2-O + O_2 → CH_3-C(=O)H (**Acetaldehyde**) + HO_2 (12b)

CH_3-CH_2-O-(C$\underline{H}$•)-CH_2-**R** + O_2 + NO → NO_2 + CH_3-CH_2-O-C(=O)H (**EF**) + •CH_2-**R** (13a)

•CH_2-**R** + O_2 → H(O=)C-**R** (**EG**) + HO_2 (13b)

CH_3-CH_2-O-(C$\underline{H}$•)-CH_2-**R** + O_2 + NO → NO_2 + CH_3-CH_2-O-C(=O)-CH_2-**R** (**DM**) (14)

For methylene III:

CH_3-CH_2-O-CH_2-C$\underline{H}_2$-**R** + OH → CH_3-CH_2-O-CH_2-C($\underline{H}$•)-**R** + H_2O (15)

CH_3-CH_2-O-CH_2-C($\underline{H}$•)-**R** + O_2 + NO → NO_2 + H(O=)C-**R** (**EG**) + CH_3-CH_2-O-CH_2• (16a)

CH_3-CH_2-O-CH_2• + O_2 + NO → NO_2 + CH_3-CH_2-O-C(=O)H (**EF**) (16b)

The major product observed was ethyl formate (EF). From the mechanism proposed, EF is a product of hydrogen abstraction from both methylene II *and* methylene III in Structure 1. The combination of two possible pathways for EF formation could explain its significantly larger yield than other reaction products. In Reaction (13a) EF is formed as an initial product of the chemical transformation of the CH_3-CH_2-O-(C$\underline{H}$•)-CH_2-**R** radical. But in Reaction (16b), EF is formed as a daughter product of the rest of

the EEP molecule after EG formation. The proposed mechanism supports the EF yield data, but there is no way to differentiate the two possible EF formation processes. The disposition of the $\bullet CH_2$-**R** fragment could lead to EG formation as well.

The next largest product yield was ethyl (3-formyloxy) propionate (EFP). The hydrogen abstraction from methylene I and subsequent reactions are similar to what was observed in the reaction of OH with 2-ethoxyethyl acetate (EEA) [24]. After hydrogen abstraction, the rest of the parent molecule remains intact, a methyl group is lost, and the formate group is formed. Unlike what was observed with EEA, there was no observed splitting between the diacetate form and the formate form of the reaction product. This may indicate the effect of the ester oxygen on the carbon backbone. For EEA, the oxygen is on the same side of the carbonyl as the radical site and may have a stabilizing effect allowing for the generation of both products, while in EEP the ester oxygen is on the other side of the carbonyl away from the hydrogen abstraction site preventing the stabilization of the radical promoting the loss of the end methyl group. The experimental technique was such that if the diacetate had been formed it would have been detected.

Ethyl glyoxate (EG) was the product with the third largest yield. Reactions (13b) and (16a) provide two possible pathways for EG formation. The structure reactivity calculation [9] predicted that 48% of the OH rate constant value could come from hyddrogen abstraction of methylene II and only 4.2% of the OH rate constant value would come from methylene III. This suggests that the Reaction (13b) is the most likely pathway for EG formation.

The last two products, ethyl (2-formyl) acetate and acetaldehyde, most likely come from the hydrogen abstraction of methylene II in Structure 1. The proposed

branched mechanistic pathway shown in Reactions 13 a and b is supported by the nearly identical yields observed for these two products. The carbon skeletal molecular structure of the two products can be summed together to form an EEP molecule which also supports the proposed mechanism.

The diethyl malonate observed in very low yield most likely came from the hydrogen abstraction of methylene II. The retention of the entire molecular "skeleton" of EEP is evident in DM's structure, and supports its proposed formation.

The linear relationship observed between products formed vs. EEP reacted indicates that EFP, EFA, EG, EF, and acetaldehyde are not lost or produced by any other side reactions. Using the atmospheric reaction mechanism proposed in Figure 12 and Reactions (9) - (16) and the product yields, approximately 72% of the carbon of the total EEP reacted is accounted. The primary error occurring from the balance of products not observed following the formation of ethyl formate in Reaction (13a) and (16b).

2. Hydroxy ether Transformation Mechanisms

OH reacts with hydroxy ethers by H-atom abstraction. Both 2EEOH and 2BEOH are molecules with several possible abstraction sites. However, the products of the reaction of OH with hydroxy ethers suggest strongly that the OH abstracts hydrogen principally from the ether methylenes. This is consistent with the reaction "hot spot" proposed by structure reactivity analysis of both 2EEOH and 2BEOH.[9] Also, the similarity between the calculated versus the measured $k_{\text{hydroxy ethers}}$ supports these "reactive site" assignments.

The experimental parameters were set to minimize other side reactions and highlight the first OH hydrogen abstraction step. Nitric oxide (NO) was added to

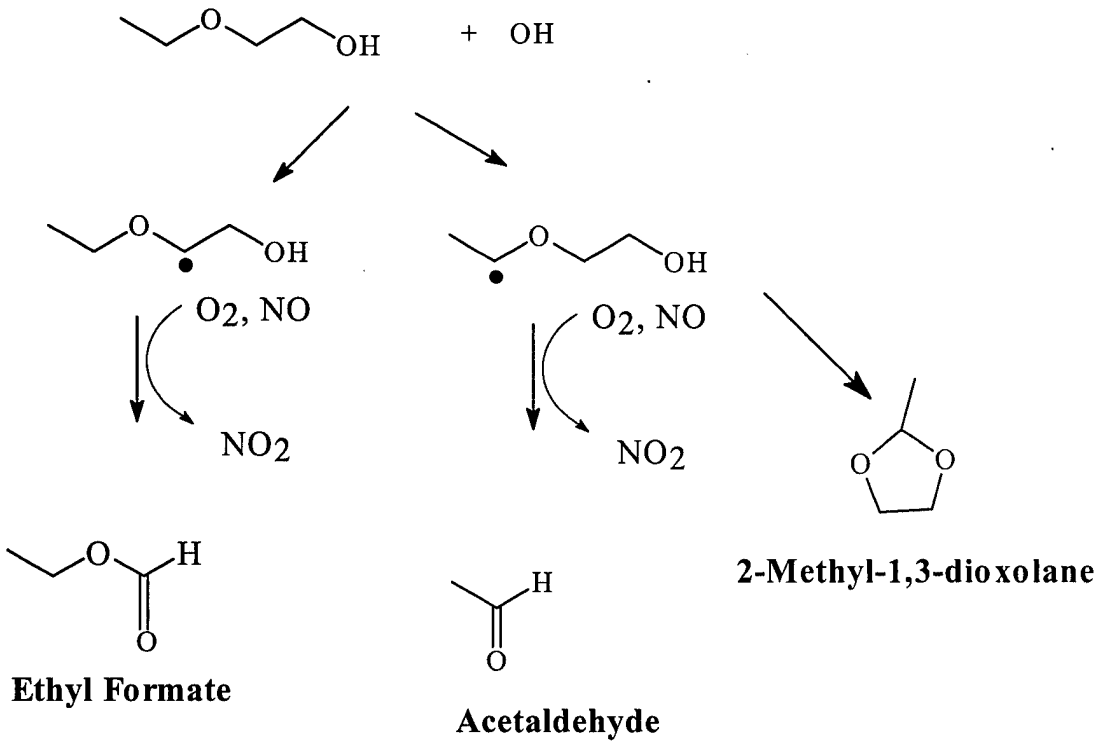

Figure 13. Proposed reaction mechanism for hydroxyl radical with 2-ethoxyethanol. Major products are labeled.

facilitate the generation of OH and to minimize ozone (O_3) and NO_3 formation preventing other possible radical reactions. The proposed OH reaction mechanisms for 2EEOH and 2BEOH are shown in Figures 13 and 14, respectively. Depending on the nature of the radical formed in Reaction (4):

For 2EEOH:

(17) $CH_3CH_2OCH_2CH_2OH + OH \rightarrow CH_3CH_2OCH(\bullet)CH_2OH + H_2O$

(18) $CH_3CH_2OCH(\bullet)CH_2OH + NO + O_2 \rightarrow\rightarrow\rightarrow CH_3CH_2OC(=O)H$ (**Ethyl formate**) (via an $RO_2\bullet$ intermediate) $+ NO_2 + \bullet CH_2OH$

(19) $CH_3CH_2OCH\bullet CH_2OH$ (decompose) $\rightarrow CH_3C(=O)H$ (**Acetaldehyde**) + $CH\bullet CH_2OH$

(20) $CH_3CH_2OCH_2CH_2OH + OH \rightarrow CH_3CH(\bullet)OCH_2CH_2OH + H_2O$

(21) $CH_3CH(\bullet)OCH_2CH_2OH + NO + O_2 \rightarrow\rightarrow\rightarrow HC(=O)CH_3$(**Acetaldehyde**) (via an $RO_2\bullet$ intermediate) $+ NO_2 + \bullet OCH_2CH_2OH$

The major product of the OH/2EEOH reaction was ethyl formate (EF, 37 ± 4%). From the mechanism proposed, EF is a product of hydrogen abstraction from methylene III in structure shown below:

CH_3-CH_2-O-CH_2-CH_2OH
I II III IV

Structure 2

The previous yield of 43 ± 10% from reference 11 is within experimental error of the yield reported here. Using structure reactivity [9], a 44% ethyl formate yield is expected. EF observation is consistent with previous studies of the hydroxyl reaction products of 2-ethoxyethyl acetate and ethyl 3-ethoxypropionate: the methylenes next to the ether oxygen are activated. [24, 33]

Acetaldehyde was observed as a product and detected using DNPH derivatization techniques. Acetaldehyde could have come from two paths: hydrogen abstraction of methylene II and as a decomposition product of hydrogen abstraction of methylene III. Reference 11 did not report acetaldehyde observations.

The 2-methyl-1,3-dioxolane product was observed using the GC/FTIR/MS system, but was not quantitated due to low yield. Reference 11 observed a dioxolane yield of 3.4 ± 2.5%. The ring forming reaction could follow hydrogen abstraction from methylene II.

However, the other oxygenated organic compounds observed in reference 11 : ethylene glycol monoformate ($HC(=O)OCH_2CH_2OH$), ethoxyacetaldehyde ($CH_3CH_2OCH_2C(=O)H$) and ethylene glycol monoacetate ($CH_3C(=O)OCH_2CH_2OH$) , were not conclusively observed. We did observe three unidentified peaks in the DNPH chromatographs, but of the products from reference 11 listed above only ethoxyacetaldehyde would be DNPH active. Comparing the yields and products reported in reference 11 and to this work and previously reported work from this laboratory indicate that there were no distinct chromatographic or sampling reasons explaining the discrepancy in product observations.

2-Butoxyethanol (2BEOH) has a similar transformation mechanism (Figure 14) to 2EEOH.

For 2BEOH:

(22) $CH_3CH_2CH_2CH_2OCH_2CH_2OH + OH \rightarrow CH_3CH_2CH_2CH_2OCH(\bullet)CH_2OH + H_2O$

(23) $CH_3CH_2CH_2CH_2OCH(\bullet)CH_2OH + O_2 + NO \rightarrow\rightarrow\rightarrow CH_3CH_2CH_2CH_2OC(=O)H$ **(Butyl formate)** (via an $RO_2\bullet$ intermediate) + NO_2 + $\bullet CH_2OH$

(24) $CH_3CH_2CH_2CH_2OCH_2CH_2OH + OH \rightarrow CH_3CH_2C(\bullet)HCH_2OCH_2CH_2OH + H_2O$

(25) $CH_3CH_2C(\bullet)HCH_2OCH_2CH_2OH + O_2 + NO \rightarrow\rightarrow\rightarrow CH_3CH_2C(=O)H$

(**Propionaldehyde**) (via an $RO_2\bullet$ intermediate) $+ NO_2 + (\bullet)CH_2OCH_2CH_2OH$

(26) $CH_3CH_2CH_2CH_2OCH_2CH_2OH + OH \rightarrow CH_3CH_2CH_2C(\bullet)HOCH_2CH_2OH + H_2O$

(27) $CH_3CH_2CH_2C(\bullet)HOCH_2CH_2OH + O_2 + NO \rightarrow\rightarrow\rightarrow CH_3CH_2CH_2C(=O)H$

(**Butyraldehyde**) (via an $RO_2\bullet$ intermediate) $+ (\bullet)OCH_2CH_2OH + NO_2$

(28) $CH_3CH_2CH_2CH_2OCH_2CH_2OH + OH \rightarrow CH_3C(\bullet)HCH_2CH_2OCH_2CH_2OH + H_2O$

(29) $CH_3C(\bullet)HCH_2CH_2OCH_2CH_2OH + NO + O_2 \rightarrow\rightarrow\rightarrow CH_3C(=O)H$

(**Acetaldehyde**) (via an $RO_2\bullet$ intermediate) $+ (\bullet)CH_2CH_2OCH_2CH_2OH + NO_2$

The major product of the OH/2BEOH reaction was butyl formate (BF, 30 ± 2%). From the mechanism proposed, BF is a product of hydrogen abstraction from methylene V in structure shown below:

CH_3- CH_2 - CH_2-CH_2-O-CH_2-CH_2OH
I II III IV V VI

Structure 3

The previous yield of 35 ± 11% from reference 12 is within experimental error of the yield reported here. Using structure reactivity [9], a 37% butyl formate yield is expected. The second major product observed was propionaldehyde (13 ± 1%). A 20-30% yield of propionaldehyde was observed in reference 12. These products and yields indicate that methylene III of EEOH and methyelene V of BEOH are major OH hydrogen abstraction sites.

Our observed yield of acetaldehyde (Reaction 29, 3.7 ± 0.4%) is consistent with the <5% yield reported in reference 12. However, the product from hydrogen abstraction at methylene IV, butyraldehyde, had an observed yield of 2.8 ± 0.2% which was larger

than <1.1% reported in reference 12. 2-Propyl-1,3-dioxolane was observed and reference 3 reported a 2.5 ± 0.5% yield.

For both 2EEOH and 2BEOH there was a significant portion of "missing" carbon. There may be several undetected nitrate products or some other product loss mechanism.

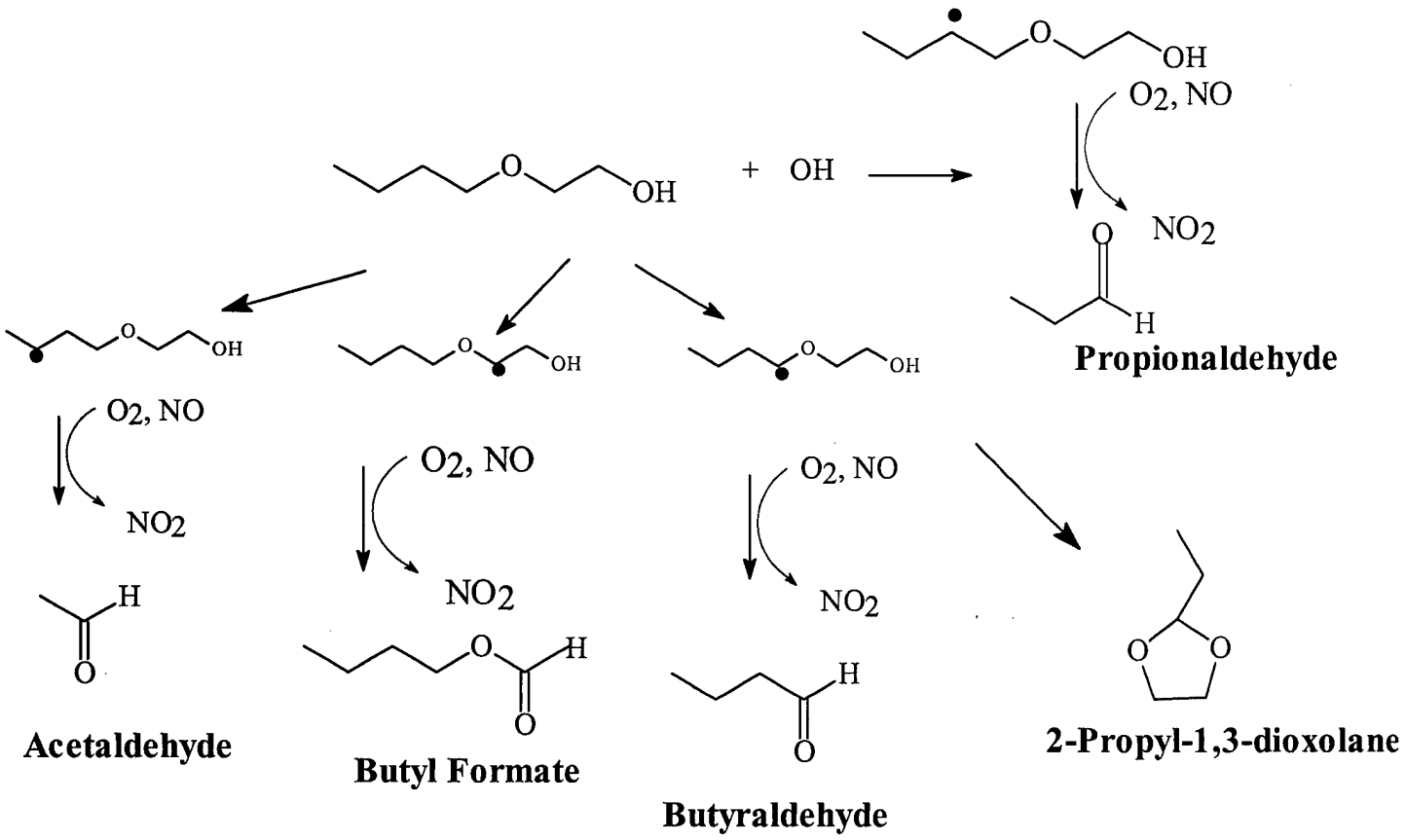

Figure 14. Proposed reaction mechanism for hydroxyl radical with 2-butoxyethanol. Major products are labeled.

OH reacts with 2PEOH by H-atom abstraction from several possible molecular sites. However, the products of the reaction of OH with 2PEOH suggest strongly that the OH abstracts hydrogen principally from the ether methylenes. This is consistent with the reaction "hot spot" proposed by structure reactivity analysis of 2PEOH.[9] Also, the similarity between the calculated versus the measured k_{2PEOH} supports these "reactive site" assignments. The k_{2PEOH} value reported in Reference 12 is somewhat smaller than the calculated value and the value reported here, but that discrepancy may be due to the OH rate constant of the reference used. The OH rate constant of 1-hexanol, the reference compound used in Stemmler *et al.*, has been recently re-measured by Aschmann *et al.*.[38] Using this new reference rate constant with k_{2PEOH} data from Reference 12 yields 20.7×10^{-12} $cm^3molecule^{-1}s^{-1}$, in excellent agreement with the reported measurement.

The experimental parameters were set to minimize other side reactions and highlight the first OH hydrogen abstraction step. Nitric oxide (NO) was added to facilitate the generation of OH and to minimize ozone (O_3) and NO_3 formation preventing other possible radical reactions. The proposed OH reaction mechanisms for 2PEOH is shown in Figure 15 and is based on products observed. Depending on the nature of the radical formed in Reaction (4):

For 2PEOH:

(30) $CH_3CH_2CH_2OCH_2CH_2OH + OH \rightarrow CH_3CH_2CH_2CH_2OCH(\bullet)CH_2OH + H_2O$

(31) $CH_3CH_2CH_2OCH(\bullet)CH_2OH + NO + O_2 \rightarrow\rightarrow\rightarrow CH_3CH_2CH_2OC(=O)H$ (**Propyl formate**) (via an $RO_2\bullet$ intermediate) $+ NO_2 + \bullet CH_2OH$

(32) $CH_3CH_2CH_2OCH_2CH_2OH + OH \rightarrow CH_3CH_2CH(\bullet)OCH_2CH_2OH + H_2O$

(33) $CH_3CH_2CH(\bullet)OCH_2CH_2OH + O_2 \rightarrow\rightarrow\rightarrow$ **2-Ethyl-1,3-dioxolane** $+ HO_2$

(34) $CH_3CH_2CH(\bullet)OCH_2CH_2OH + O_2$ (alcoholic hydrogen shift) $\rightarrow\rightarrow\rightarrow$ $CH_3CH_2CH_2OCH_2CH(=O)$ (**2-Propoxyethanal**) $+ HO_2$

(35) $CH_3CH_2CH_2OCH_2CH_2OH + OH \rightarrow CH_3CH_2CH_2OCH_2CH(\bullet)OH + H_2O$

(36) $CH_3CH_2CH_2OCH_2CH(\bullet)OH + O_2 \rightarrow CH_3CH_2CH_2OCH_2CH(=O)$ (**2-Propoxyethanal**) $+ HO_2$

The major product of the OH/2PEOH reaction was propyl formate (PF, 47 ± 2%). From the mechanism proposed, PF is a product of hydrogen abstraction from methylene IV in the structure shown below:

CH_3-CH_2-CH_2-O-CH_2-CH_2OH
I II III IV V

Structure 4

Using structure reactivity [9], a 39 % propyl formate yield is expected. PF observation is consistent with previous studies of the hydroxyl reaction products of 2-ethoxyethyl acetate and ethyl 3-ethoxypropionate: the methylenes next to the ether oxygen are activated. [11, 14, 24, 33, 35]

The 2-ethyl-1,3-dioxolane (5.4 ± 0.4 %) product was observed using the GC/MS system and is formed from abstraction of the methylene III. While using structural reactivity a 39 % yield of hydrogen abstraction from methylene III is expected. The dioxolane yield is far from 39 %. However, the radical could transfer a hydrogen from the alcohol (Reaction 34), open up and form 2-propoxyethanal.

Hydrogen abstraction from methylene V (Reactions 35 and 36) and alcoholic hydrogen abstraction (Reaction 34) are the most likely routes for 2-propoxyethanal formation. A 16 % reaction probability was calculated from structural reactivity for

methylene V and is consistent for the 2-propoxyethanal yield observed. [9] The correlation between the calculated and observed 2-propoxyethanal yield suggests that its formation via Reaction 34 is less likely.

In summary, approximately 67% of the reaction pathways have been identified. The bulk of the unobserved products or pathways most likely come from reactions pertaining to the $CH_3CH_2CH(\bullet)OCH_2CH_2OH$ radical. As stated above, the low dioxolane yield is inconsistent with the calculated reactive nature of the methylene radical sight. Other potential products from isomerization or decomposition of the $CH_3CH_2CH(\bullet)OCH_2CH_2OH$ radical include $CH_3CH_2CH(O\bullet)OCH_2CH_2OH$, $CH_3CH_2C(=O)OCH_2CH_2OH$, $CH(=O)OCH_2CH_2OH$, and $CH_3C(=O)H$ (acetaldehyde). Acetaldehyde was not detected using the same DNPH derivatization techniques that have previously detected it. Either the other possible products were not formed or were not detected. Previous investigations from this laboratory suggest that some of the products mentioned above could have been detected. However, other processes such as wall loss or nitrate formation could account for their absence.

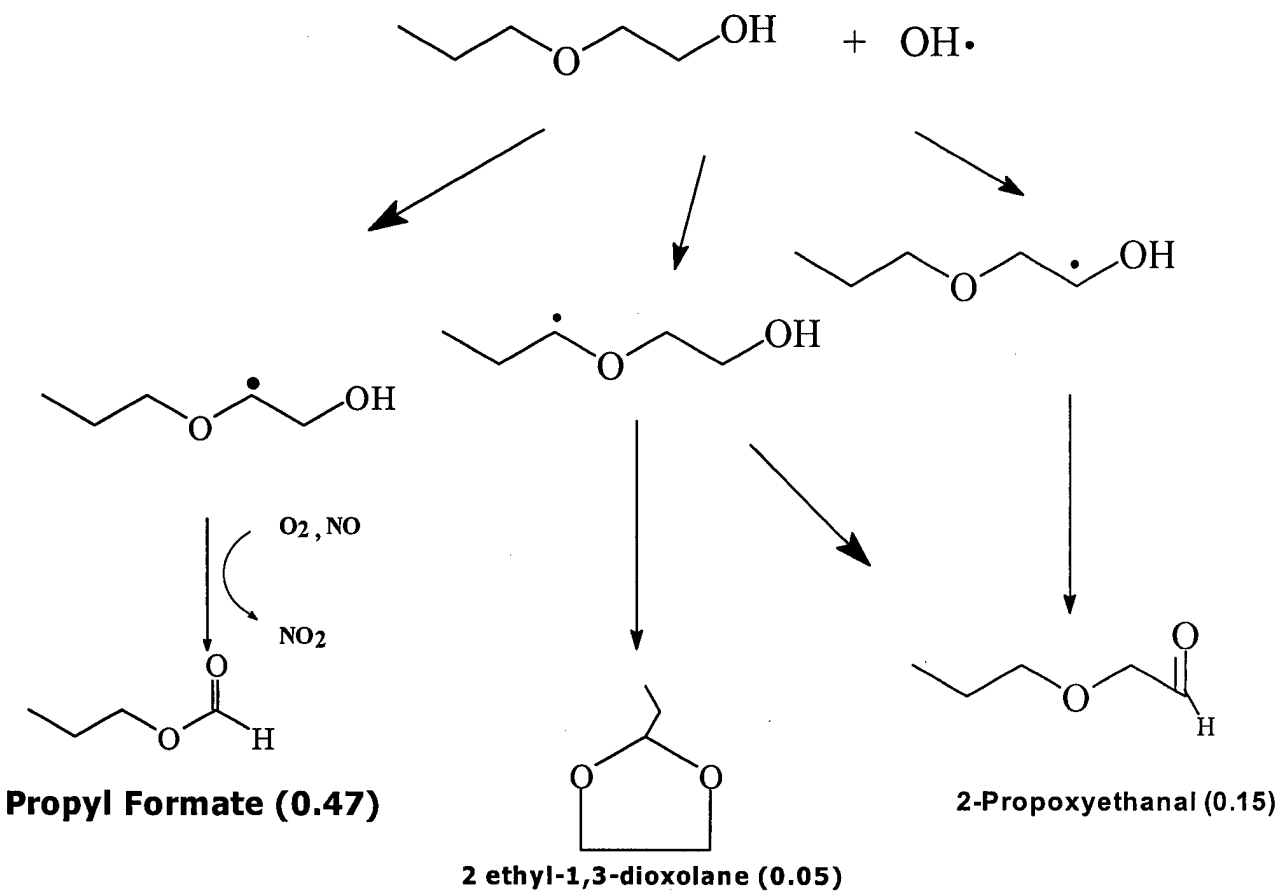

Figure 15. Proposed reaction mechanism for hydroxyl radical with 2-propoxyethanol. Major products are labeled with yield in parentheses.

3. Secondary Alcohol Transformation Mechansims

OH reacts with alcohols by H-atom abstraction and both 2BU and 2PE are molecules with several possible abstraction sites. However, the products of the reaction of OH with alcohols strongly suggest that the OH abstracts hydrogen principally from the alcoholic carbon. This is consistent with the reaction "hot spot" proposed by structure reactivity analysis of both 2BU and 2PE.[9] Also, the agreement between the calculated versus the measured $k_{alcohols}$ supports these "reactive site" assignments. However, the structure reactivity *calculated* MEK and 2-pentanone yields were 84% and 76% respectively. The lower *observed* ketone yields, 60% (MEK) and 41% (2-pentanone), reported here and in reference [16] suggests the –OH activating effects are less than assumed by structure reactivity calculations and/or due to competition for acetaldehyde and propionaldehyde formation.

The proposed OH reaction mechanisms for 2BU and 2PE are shown below. Depending on the nature of the radical formed in Reaction (4):

For 2BU:

(37a) $CH_3CH_2CH(OH)CH_3 + OH \rightarrow CH_3CH_2C\bullet(OH)CH_3 + H_2O$

(37b) $CH_3CH_2CH(OH)CH_3 + OH \rightarrow CH_3C\bullet HCH(OH)CH_3 + H_2O$

(38a) $CH_3CH_2C\bullet(OH)CH_3 + O_2 \rightarrow CH_3CH_2C(=O)CH_3$(**MEK**) $+ HO_2$

(38b) $CH_3CH_2C\bullet(OH)CH_3$ (decompose) $\rightarrow CH_3CH_2\bullet + HC(=O)CH_3$(**Acetaldehyde**)

(39) $CH_3CH_2\bullet + NO + O_2 \rightarrow\rightarrow\rightarrow HC(=O)CH_3$(**Acetaldehyde**) (via an $RO_2\bullet$ intermediate) $+ NO_2$

(40) $CH_3C\bullet HCH(OH)CH_3 + NO + O_2 \rightarrow\rightarrow\rightarrow HC(=O)CH_3$(**Acetaldehyde**) (via an $RO_2\bullet$ intermediate) $+ NO_2$

The major product of the OH/2BU reaction was methyl ethyl ketone (MEK (60 ± 2)%). From the mechanism proposed, MEK is a product of the hydrogen abstraction from the alcoholic carbon. Using ^{18}O labeled 2BU and mass spectral analysis of OH + 2BU reaction products, insights into the details of the $CH_3CH_2C\bullet(^{18}OH)CH_3$ radical reaction pathway could be investigated. The MEK product from reaction 38a was pure ^{18}O labeled. This result confirms retention of the alcoholic oxygen in the product and means that atmospheric oxygen (mainly $^{16}O_2$) does not play a role in the reaction mechanism. If atmospheric oxygen was involved in MEK formation, the MEK product would either be mixed $^{18}O/^{16}O$ or pure ^{16}O, neither of which was observed. This finding is instructive for assessing the incremental reactivity (ozone-forming potential) of 2BU and possibly other aliphatic alcohols. Tropospheric ozone is a by-product of the oxidation of volatile organic compounds (VOCs) [1]. The ^{18}O experiment provides definitive evidence that the $CH_3CH_2C\bullet(OH)CH_3$ radical/atmospheric oxygen reaction does not yield a tropospheric ozone-forming $RO_2\bullet$ type radical.[1] To our knowledge, this is the first direct confirmation of the retention of the alcoholic oxygen in the reaction product.

The other reaction product, acetaldehyde, was observed by DNPH derivatization. The acetaldehyde could have come from decomposition (Reactions 38b and 40) and reaction of the $CH_3CH_2\bullet$ radical (Reaction 39). The detection method used could not distinguish between different acetaldehyde pathways.

2-Pentanol (2PE) more than likely has similar mechanistic pathways as 2BU discussed above.

For 2PE:

(41a) $CH_3CH_2CH_2CH(OH)CH_3 + OH \rightarrow CH_3CH_2CH_2C\bullet(OH)CH_3 + H_2O$

(41b) $CH_3CH_2CH_2CH(OH)CH_3 + OH \rightarrow CH_3CH_2C\bullet HCH(OH)CH_3 + H_2O$

(41c) $CH_3CH_2CH_2CH(OH)CH_3 + OH \rightarrow CH_3C\bullet HCH_2CH(OH)CH_3 + H_2O$

(42) $CH_3CH_2CH_2C\bullet(OH)CH_3 + O_2 \rightarrow CH_3CH_2CH_2C(=O)CH_3$ (**2-Pentanone**) + HO_2

(43) $CH_3CH_2CH_2C\bullet(OH)CH_3 + NO + O_2$ (decompose) $\rightarrow\rightarrow\rightarrow$ $CH_3CH_2C(=O)H$ (**propionaldehyde**) (via an $RO_2\bullet$ intermediate) + $CH_3C(=O)H$ (**acetaldehyde**) (via an $RO_2\bullet$ intermediate) + NO_2

(44) $CH_3CH_2C\bullet HCH(OH)CH_3 + NO + O_2$ (decompose) $\rightarrow\rightarrow\rightarrow$ $CH_3CH_2C(=O)H$ (**propionaldehyde**) (via an $RO_2\bullet$ intermediate) + $CH_3C(=O)H$ (**acetaldehyde**) (via an $RO_2\bullet$ intermediate) + NO_2

(45) $CH_3C\bullet HCH_2CH(OH)CH_3 + NO + O_2$ (decompose) $\rightarrow\rightarrow\rightarrow$ $CH_3C(=O)H$ (**acetaldehyde**) (via an $RO_2\bullet$ intermediate)+ NO_2 + unobserved products

The major product, 2-pentanone, is expected to be formed the same way as the MEK product in the 2BU mechanism above. The smaller yield of 2-pentanone, compared to structure reactivity calculations, could be due in part to the multiple reaction/decomposition pathways for the $CH_3CH_2CH_2C\bullet(OH)CH_3$ radical and more OH reactive sites on 2PE. The multiple radical pathways leading to product are probably due to the stability of this larger radical. The same implication regarding the effect of ketone yield data on incremental reactivity that was made for 2BU above can be made for 2PE.

The pathways for propionaldehyde and acetaldehyde formation are not as straightforward as 2-pentanone's. The combination of acetaldehyde and propionaldehyde carbon structures yields a five carbon backbone like 2PE. At first inspection, the yields of acetaldehyde and propionaldehyde might be expected to be the same if both were

formed from decomposition of the same 2PE molecule. However, the yields of propionaldehyde ((14 ± 2)%) and acetaldehyde ((40 ± 4)%) are significantly different to suggest each product may have multiple formation routes. As the carbon backbone lengthens the possibility of isomerization increases. [39, 40] The primary radical can self abstract hydrogen and open the door to several alternative reaction paths resulting in products that are not simple straight chain aldehydes and ketones such as cyclic compounds, diols and others. As can be seen from the mechanism proposed, there are several routes for propionaldehyde and acetaldehyde formation. More labeling experiments to sort these transformation pathways are needed to clarify these mechanisms. Also, experiments to determine nitrate reaction product transformation pathways are needed to more fully understand organic compounds' atmospheric mechanisms.

4. IBA/OH Reaction Mechanism

OH reacts with IBA by H-atom abstraction. IBA is a large molecule with *five* possible carbons as hydrogen abstraction sites. However, both SAR calculations and observed OH/IBA reaction products suggest that the OH abstracts hydrogen principally from *two* molecular sites; carbon III and methylene IV using Structure 5 below.[9]

$(CH_3)_2CHCH_2$-O-C(=O)CH_3
I,II III IV V

Structure 5

The agreement between the calculated versus the measured k_{IBA} supports these "reactive site" assignments.

The experimental parameters were set to minimize other side reactions and highlight the first OH hydrogen abstraction step. Nitric oxide (NO) was added to

facilitate the generation of OH and to minimize ozone (O_3) and NO_3 formation preventing other possible radical reactions. After hydrogen abstraction from IBA by the OH radical:

For carbon III:

(46a) $(CH_3)_2C\bullet CH_2\text{-}O\text{-}C(=O)CH_3 + O_2 + NO \text{ ---> } (CH_3)_2C(=O)$ (**Acetone**) + $\bullet CH_2\text{-}O\text{-}C(=O)CH_3$ (?)+ $NO_2 + HO_2$

(46b) $\bullet CH_2\text{-}O\text{-}C(=O)CH_3 + O_2 + NO \text{ ----> } H(O=)C\text{-}O\text{-}C(=O)CH_3 + NO_2 + HO_2$

For methylene IV:

(47a) $(CH_3)_2CH_2CH\bullet\text{-}O\text{-}C(=O)CH_3 + O_2 + NO \text{ --> } (CH_3)_2CHC\bullet + HOC(=O)CH_3$ (**Acetic acid**) + $HO_2 + NO_2$

(47b) $(CH_3)_2CHC\bullet + O_2 + NO \text{ --> } (CH_3)_2C(=O)$ (**Acetone**)

(48) $(CH_3)_2CH_2CH\bullet\text{-}O\text{-}C(=O)CH_3 + O_2 + NO \text{ --> } (CH_3)_2CH_2C(=O)\text{-}O\text{-}C(=O)CH_3 + HO_2 + NO_2$

The major product observed was acetone. From the mechanism proposed, acetone could be a product of hydrogen abstraction from both carbon III *and* methylene IV, Reactions 46a and 47b, respectively. Acetone formed from hydrogen abstraction at carbon III correlated with the SAR calculations implicating carbon III's contribution to the total k_{IBA} as greater than 51%. [9]; the observed acetone yield of 62% is another supporting indicator of the SAR calculation. Therefore, Reaction 46a is most likely the major acetone formation pathway. It is conceivable that acetone could be formed from other transformation reactions (Reaction 47b). The other proposed product of Reaction 8b, $H(O=)COC(=O)CH_3$, was not observed, but it might not be stable and "decompose" to yield acetic acid and carbon monoxide. Nonetheless, its disposition is not known and there are no molecular fragments to suggest its fate.

As mentioned in the Results section, acetic acid was also observed but was very difficult to quantitate and its yield could not been determined. However, identification of acetic acid does suggest a reaction pathway centered at methylene IV(Reaction 47a) or as mentioned above as a decomposition product of $H(O=)COC(=O)CH_3$. Methylene IV was the second largest contributor to the SAR calculated rate constant (39%). The disposition of the $(CH_3)_2CHC\bullet$ radical could result in the formation of more acetone (Reaction 47b) or it could "decompose" into smaller molecular fragments. Reaction 48 is included for completeness and the chromatographic system used should be able to detect it. However, it was not observed and it may also have decomposed into smaller or undetectable fragments. The lack of newly observed DNPH derivatized hydrozones suggests that no other aldehydes or ketones are formed from the reaction of OH with IBA.

The release of IBA into the atmosphere may have air quality impacts if the proposed mechanistic steps are true. Reactions 8a and 8b are pathways for 1 OH radical hydrogen abstraction step to result in the conversion of *2* NO molecules to *2* NO_2 molecules which ultimately forms *2* O_3 molecules.[1]. Therefore a detailed investigation into the maximum incremental reactivity of this compound is warranted to more fully understand the air quality impact of IBA.[7]

5. HXA/OH Reaction Products

OH reacts with HXA by H-atom abstraction. HXA is a large molecule with *seven* possible carbons as hydrogen abstraction sites. The reaction product yields as mentioned in the Results section, do not nearly account for the loss of HXA, but their discovery highlights interesting atmospheric transformation pathways. The observed OH/HXA

reaction products and SAR calculations suggest that the OH hydrogen abstraction occurs principally from *five* groups (II - VI in Structure 6 below). [9]

$CH_3CH_2CH_2CH_2CH_2CH_2$-O-C(=O)CH_3

I II III IV V VI VII

Structure 6

The experimental parameters were set to minimize other side reactions and highlight the first OH hydrogen abstraction step. Nitric oxide (NO) was added to facilitate the generation of OH and to minimize ozone (O_3) and NO_3 formation preventing other possible radical reactions

For methylene II:

(49) $CH_3C(\bullet)HCH_2CH_2CH_2CH_2$-O-C(=O)$CH_3 + O_2 + NO$ --->

$CH_3C(=O)CH_2CH_2CH_2CH_2$-O-C(=O)$CH_3$ (***5-hexanone acetate***) + $HO_2 + NO_2$

For methylene III:

(50a) $CH_3CH_2C(\bullet)HCH_2CH_2CH_2$-O-C(=O)$CH_3 + O_2 + NO$ ---> $CH_3CH_2C(=O)$

$CH_2CH_2CH_2OC(=O)CH_3$ (***4-hexanone acetate***) + $HO_2 + NO_2$

(50b) $CH_3CH_2C(\bullet)HCH_2CH_2CH_2$-O-C(=O)$CH_3 + O_2 + NO$ ---> $HC(=O)CH_2CH_2CH_2$-O-

$C(=O)CH_3 + HO_2 + NO_2$

For methylene IV:

(51) $CH_3CH_2CH_2C(\bullet)HCH_2CH_2$-O-C(=O)$CH_3$ ---> **α-methylpropyl-γ-butyrolactone**

For methylene V:

(52) $CH_3CH_2CH_2CH_2C(\bullet)HCH_2$-O-C(=O)$CH_3$ ---> **β-butyl-γ-butyrolactone**

For methylene VI

(53a) $CH_3CH_2CH_2CH_2CH_2C(\bullet)H$-O-C(=O)$CH_3$ ---> H-O-C(=O)CH_3 (**Acetic Acid**) +

$CH_3CH_2CH_2CH_2CH_2C(\bullet)$

(53b) $CH_3CH_2CH_2CH_2CH_2C(\bullet)H\text{-}O\text{-}C(=O)CH_3 + O_2 + NO \rightarrow$

$CH_3CH_2CH_2CH_2CH_2C(=O)H$ (**Hexanal**)

The observed products were in very low concentrations. Due to the same chromatographic limitations discussed for IBA, acetic acid was not quantitated. The longer acetate, having more hydrogen abstraction sites, has several reaction pathways yielding the observed broad spectrum of transformation products.

Even though the carbon balance is poor, the sheer variety of products observed is crucial to understanding the air quality impacts of HXA. Of the seven steps proposed to account for the observed products one in an NO sink, two are ring closing reactions and the rest involve NO to NO_2 conversion to make the aldehyde or ketone product. [1] The ring closing reaction products could be nuclei for particulate matter, also a regulated pollutant. [41] Therefore a detailed investigation into the maximum incremental reactivity of HXA is warranted to more fully understand its air quality impact.[7]

6. Methyl isobutyrate Transformation Mechanism

OH reacts with MIB by H-atom abstraction. MIB is a large molecule with four possible carbons as hydrogen abstraction sites. However, the products of the reaction of OH with MIB suggest strongly that the OH abstracts hydrogen principally from *one* reaction site (group III below). The "reactive structure" of MIB can be drawn as shown in Structure 7:

$$\underset{\text{I,II}}{(C\underline{H}_3)_2} - \underset{\text{III}}{C\underline{H}} - C(=O) - O - \underset{\text{IV}}{C\underline{H}_3}$$

Structure 7

This is consistent with the reaction mechanisms proposed for tertiary hydrocarbons and consistent as the site having the largest contribution to the calculated k_{MIB} using structure

reactivity [9]. Also, the agreement between the calculated versus the measured k_{MIB} supports this "reactive site" assignment.

The experimental parameters were set to minimize other side reactions and highlight the first OH hydrogen abstraction step. Nitric oxide (NO) was added to facilitate the generation of OH and to minimize ozone (O_3) and NO_3 formation preventing other possible radical reactions. The proposed OH reaction mechanism is shown in Figure 16. Depending on the nature of the radical formed in Reaction (4):

For hydrocarbon III:

$(CH_3)_2$-C<u>H</u>-C(=O)-O-CH_3 + OH → $(CH_3)_2$-(C•)-(C=O)-O-CH_3 + H_2O (54)

$(CH_3)_2$-(C•)-(C=O)-O-CH_3 + O_2 + NO → $(CH_3)_2$-C=O (**Acetone**) + •(C=O)-O-CH_3 + NO_2 (55a)

$(CH_3)_2$-(C•)-(C=O)-O-CH_3 + O_2 + NO → $CH_3C(=O)C(=O)OCH_3$(**MP**) + NO_2 + •CH_3 (55b)

For methyls I and II:

(C<u>H</u>$_3)_2$-CH-C(=O)-O-CH_3 + OH → $CH_3(CH_2•)$-CH -(C=O)-O-CH_3 + H_2O (56)

$CH_3(CH_2•)$-CH -(C=O)-O-CH_3 (decompose) → CH_3-(CH•) -(C=O)-O-CH_3 + $(CH_2•)$ (57)

CH_3-(CH•) -(C=O)-O-CH_3 + $2O_2$ + NO → CH_3-(C=O) -(C=O)-O-CH_3 (**MP**)+ HO_2 + NO_2 (58)

The major product observed was acetone. From the mechanism proposed, it is formed from hydrogen abstraction from hydrocarbon III Structure 7.

Methyl pyruvate (MP) was the other product observed. There are two possible reaction pathways, but the most probable one is hydrogen abstraction from hydrocarbon III. MP was observed as a product from the reaction of the hydroxyl radical with methyl lactate ($CH_3C(OH)HC(=O)OCH_3$). [42]

The linear relationship observed between products formed vs. MIB reacted indicates that acetone and MP are not lost or produced by any other side reactions. Using the atmospheric reaction mechanism proposed in Figure 16 and Reactions (54) - (58) and

the product yields, approximately 60% of the carbon of the total MIB reacted is identified. The primary source of unidentified carbon is probably the balance of products not observed following the formation of the $\bullet C(=O)OCH_3$ radical formed in Reaction 55a.

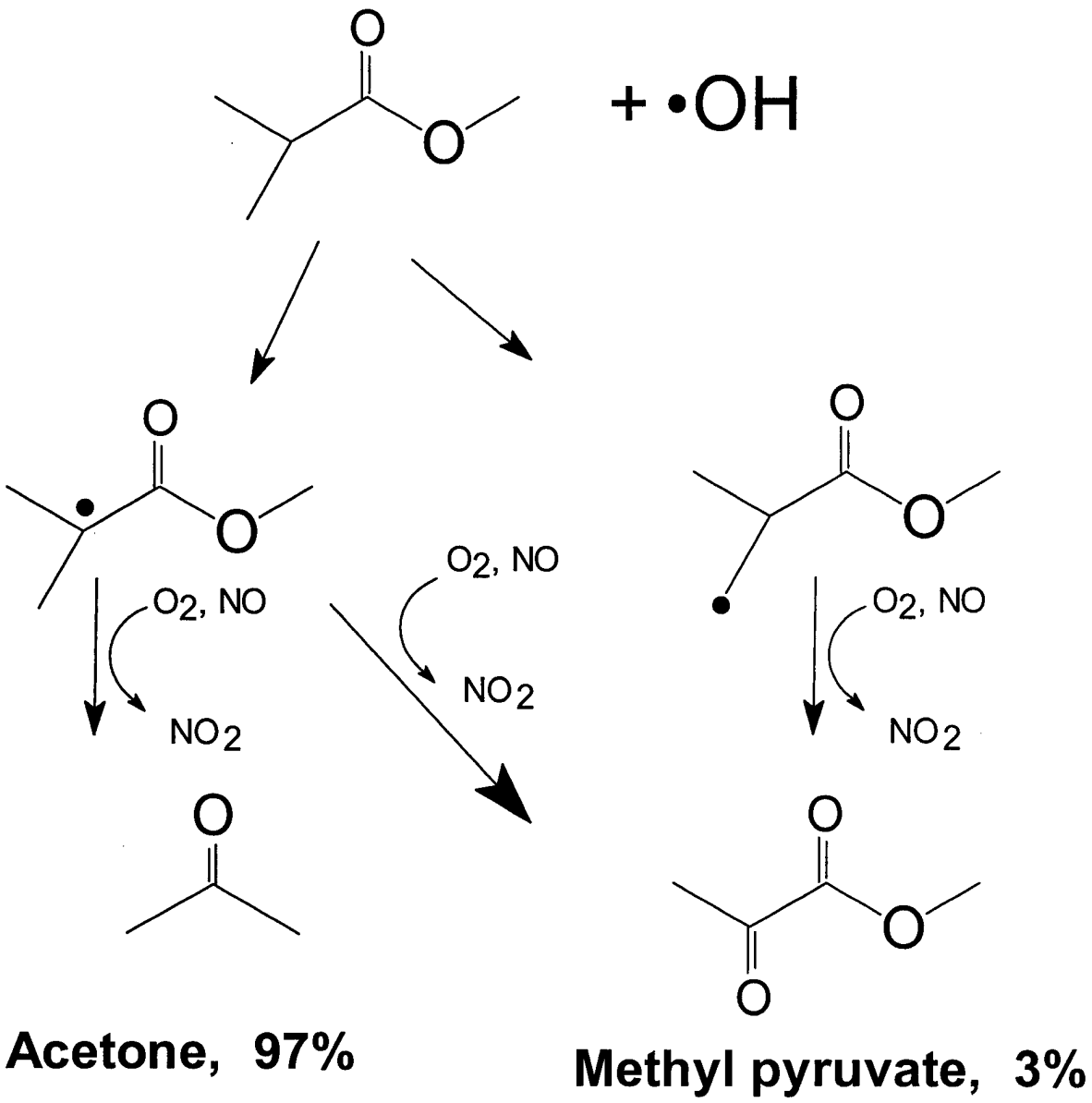

Figure 16. Proposed reaction mechanism for hydroxyl radical with methyl isobutyrate. Major products are in bold typeface.

7. Siloxane Transformation Mechanisms

OH reacts with MM, MDM, and MD_2M by H-atom abstraction from a methyl group attached to the silicon [20, 21, 36]. The reaction mechanisms, based upon the observed products are proposed in reactions (59) through (72). The formation of cyclic siloxane compounds from MDM and MD_2M present interesting mechanistic pathways where the RO_2 siloxane folds back on itself, loses a methyl group and adds an oxygen-silicon bond.

The experimental parameters were set to minimize other side reactions and highlight the first OH hydrogen abstraction step. Nitric oxide (NO) was added to facilitate the generation of OH and to quench ozone (O_3) formation and thus prevent unnecessary side reactions. However, siloxane/O_3 reaction rates have been shown to be negligible [20]. The OH generation was controlled by minimizing the total photolysis time so that only 20-30% of the siloxane was removed by reaction with the hydroxyl radical. The following mechanisms are proposed for the formation of OH + siloxane reaction products:

a. Mechanism for MM

(59) $OH + (CH_3)_3Si\text{-}O\text{-}Si(CH_3)_3 \rightarrow CH_2(CH_3)_2Si\text{-}O\text{-}Si(CH_3)_3 + H_2O$

(60) $CH_2(CH_3)_2Si\text{-}O\text{-}Si(CH_3)_3 + O_2 \rightarrow OOCH_2(CH_3)_2Si\text{-}O\text{-}Si(CH_3)_3$

(61) $OOCH_2(CH_3)_2Si\text{-}O\text{-}Si(CH_3)_3 + NO \rightarrow OCH_2(CH_3)_2Si\text{-}O\text{-}Si(CH_3)_3 + NO_2$

(62) $OCH_2(CH_3)_2Si\text{-}O\text{-}Si(CH_3)_3 + O_2 \rightarrow OCHO(CH_3)_2Si\text{-}O\text{-}Si(CH_3)_3 + ?$

(63) $OCHO(CH_3)_2Si\text{-}O\text{-}Si(CH_3)_3 + H_2O \rightarrow HO(CH_3)_2Si\text{-}O\text{-}Si(CH_3)_3$ (**MDOH**) + HC(O)OH

Reaction (63) has been proposed by Atkinson *et al.* [20]. The ester ($OCHO(CH_3)_2Si$-O-$Si(CH_3)_3$) was proposed as the product responsible for the data observed in their atmospheric pressure ionization mass spectral (API MS/MS) and long path FTIR experiments. However, water in the atmosphere would drive reaction (63) so that while MDOH is a "second generation" product, it is likely to be the important product from the atmospheric transformation of MM. The data presented here supports this fact as the observed product MDOH is in ~70% yield.

b. Mechanism for MDM

The first step of this mechanism, the removal of a hydrogen from a methyl group by OH, will be left out for brevity. The $\underline{\check{S}}$ will be defined as the rest of the siloxane molecule.

Formation of both MD_2OH and M_2TOH most likely have a very similar mechanisms:

(64) $CH_2\underline{\check{S}} + O_2 \rightarrow OOCH_2\text{-}\underline{\check{S}}$

(65) $OOCH_2\text{-}\underline{\check{S}} + NO \rightarrow OCH_2\text{-}\underline{\check{S}} + NO_2$

(66) $OCH_2\text{-}\underline{\check{S}} + O_2 \rightarrow OCHO\text{-}\underline{\check{S}}$

(67) $OCHO\text{-}\underline{\check{S}} + H_2O \rightarrow HO\text{-}\underline{\check{S}}$ **(MD_2OH and M_2TOH)**

Formation of the cyclic compound requires the addition of an oxygen molecule to an open site on the silicon and the loss of a methyl group as the ring closes. In the gas phase: ($\underline{Si} = (CH_3)_2Si$)

(68) $CH_2\underline{Si}\text{-}O\text{-}\underline{Si}\text{-}O\text{-}\underline{Si}(CH_3) + O_2 \rightarrow OOCH_2\underline{Si}\text{-}O\text{-}\underline{Si}\text{-}O\text{-}\underline{Si}(CH_3)$

(69) $OOCH_2\underline{Si}\text{-}O\text{-}\underline{Si}\text{-}O\text{-}\underline{Si}(CH_3) + NO \rightarrow OCH_2\underline{Si}\text{-}O\text{-}\underline{Si}\text{-}O\text{-}\underline{Si}(CH_3) + NO_2$

(70) $OCH_2\underline{Si}\text{-}O\text{-}\underline{Si}\text{-}O\text{-}\underline{Si}(CH_3) \rightarrow \underline{Si}\text{-}O\text{-}\underline{Si}\text{-}O\text{-}\underline{Si}(CH_3) + CH_2O$

(71) $\underline{Si}\text{-}O\text{-}\underline{Si}\text{-}O\text{-}\underline{Si}(CH_3) + O_2 \rightarrow OO\underline{Si}\text{-}O\text{-}\underline{Si}\text{-}O\text{-}\underline{Si}(CH_3)$

(72) $OO\underline{Si}\text{-}O\text{-}\underline{Si}\text{-}O\text{-}\underline{Si}(CH_3) \xrightarrow{-CH_3,-O} ((CH_3)_2Si\text{-}O)_3)$

This rearrangement could also be the product of a surface reaction. The observation of ocatmethylcyclotetrasiloxane ($(((CH_3)_2Si\text{-}O)_4$) as a "product" suggests a surface mechanism in which another $Si(CH_3)_2$ is added to the parent siloxane. The possibility of this occurring in the gas phase is remote due to the lower concentrations of the first generation reaction products.

The reaction mechanism for MD_2M is difficult to interpret due to the poor correlations between observed products' concentrations versus loss of MD_2M. Here again, surface reactions may play a role and cloud useful gas phase mechanistic information.

SECTION IV

CONCLUSIONS

The newly revised tighter air quality regulations for particulate matter and regional ozone have emphasized the need to characterize emissions of painting, depainting, cleaning, fueling and other operations. Substituting chlorinated and organic solvents has been an important technique to meet the regulatory challenges. Oxygenated organics have shown great promise as a new class of solvents. However their impact on the atmosphere is not very well known. The data presented in this report is useful to prevent unnecessary regulatory burdens.

The most reactive sites on the molecules were the methylenes connected to the ether oxygens. The hydroxyl radical rate constants in Table 1 and reaction mechanisms demonstrate the wide range of reactive properties. Currently, Material Safety Data Sheets (MSDS) do not provide the data necessary to assess presently used and potential substitute formulations. Preventing unforeseen regulatory burdens will become more important as decisions are made for new substitutes and new regulations are implemented.

Formulation selection decisions based solely on MSDS data can result in unnecessary health and regulatory burdens. Formulation composition is not equivalent to formulation emissions. Formulation emission profiles can be radically different from MSDS formulation data. For example, a non-MSDS listed small percentage chemical may constitute the bulk of the emissions for the formulation. If this chemical is a significant source of ground level ozone or particulate matter, a more educated decision can be made regarding formulation use.

This new and vital information will be used to direct the research of the atmospheric assessment program.

REFERENCES

1. Seinfeld, J.H., Science, vol 243, 1989, 745.

2. Smith, D.F.; Kleindienst, T.E.; Hudgens, E.E.; Bufalini, J.J. International Journal of Environmental Analytical Chemistry, vol 54, 1994, 265.

3. Atkinson, R.;Carter, W.P.L.; Winer, A.M.; and Pitts, J.N., Journal of Air Pollution Control, vol 31, 1981, 1090.

4. Taylor, W.D.; Allston, D.; Moscato, M.J.; Fazekas, G.D.; Kozlowski, R.; Tkacs, G.A., International Journal of Chemical Kinetics, vol 12, 1980, 231.

5. Smith, D.F.;Kleindienst, T.; Hudgens, E.E., Journal of Chromatography, vol 483, 1989, 431.

6. Finlayson-Pitts, B.J.; Pitts, Jr., J.N. Journal of the Air and Waste Management Association, vol 43, 1993, pp. 1091.

7. Carter, W.P.L., Journal of the Air and Waste Management Association, vol 44, 1994,. 881.

8. Atkinson, R., Journal of Physical and Chemical Reference Data (Monograph No. 2), 1994.

9. Kwok, E.S.C. and Atkinson, R. Atmospheric Environment, vol 29, 1995, 1685.

10. Dagaut, P.; Liu, R.; Wallington, T.J.; Kurylo, M.J. Journal of Physical Chemistry, vol 93, 1989, 7838.

11. Stemmler, K.; Mengon, W.; Kerr, J. A. Environmental Science and Technology, vol 30, 1996, 3385.

12. Stemmler, K.; Kinnison, D. J.; Kerr, J. A. Journal of Physical Chemistry vol 100, 1996, 2114.

13. Harmann, D.; Greda, A.; Rhäsa, D.; Zellner, R. Proceedings of the European Symposium on Physico-Chemical Behaviour of Atmospheric Pollutants; Riedel: Dordrecht, The Netherlands, 1987.

14. Stemmler, K.; Mengon, W.; Kinnison, D. J.; Kerr, J. A. Environmental Science and Technology, vol 31, 1997, 1496.

15. Aschmann, S.M.; Atkinson, R. submitted to International Journal of Chemical Kinetics.

16. Chew, A. A.; Atkinson, R. Journal of Geophysical Research, vol 101, 1996, 28649.

17. Wallington ,T.J; Dagaut, P.; Liu, R.; Kurylo, M. J. International Journal of Chemical Kinetics, vol 20, 1988, 541.

18. Boudali, A.E.; LeCalvé, S.; LeBras, G.; and Mellouki, A.; Journal of Physical Chemistry, vol 100, 1996, 12364.

19. Williams, D.C.; O'rji, L.N; Stone, D.A. International Journal of Chemical Kinetics, vol 25, 1993, 539.

20. Atkinson R,. Environmental Science and Technology,. vol 25, 1991, 863.

21. Sommerlade R.; Parlar, H.; Wrobel, D.; Kochs, R. Environmental Science and Technology, vol 27, 1993, 2435.

22. Smith, D.F.; McIver, C.D.; Kleindienst, T.E. International Journal of Chemical Kinetics, vol 27, 1995, 453.

23. Atkinson, R.; Aschmann, S.M.; Carter, W.P.L.; Winer, A.M.; and Pitts, J.N., Jr. Journal of Physical Chemistry, vol 86, 1982, 4563.

24. . Wells, J.R.; Wiseman, F.L.; Williams, D.C.; Baxley, J.S.; Smith, D.F.; International Journal of Chemical Kinetics, vol 28, 1996, 475.

25. Smith, D.F.; Kleindienst,T.E.; Hudgens, E.E.; McIver, C.D.; Bufalini, J.J.; International Journal of Chemical Kinetics, vol 24, 1992, 199.

26. Wallington, T.J.; Andino, J.M.; Potts, A.R.; Rudy, S.J.; Siegl, W.O.; Zhang, Z.; Kurylo, M.J.; Huie, R.E. Environmental Science and Technology, vol 27, 1993, 98.

27. Wallington, T.J.; Dagaut, P.; Liu, R.; and Kurylo, M.J. International Journal of Chemical Kinetics, vol 27, 1988, 177.

28. Niki, H.; Maker, P.D.; Savage, C.M.; Breitenbach, L.P.; Journal of Physical Chemistry, vol 82, 1978, 132.

29. Atkinson, R.; Pitts, J.N., Jr, Journal of Chemical Physics, vol 68, 1978, 3581.

31. Michael, J.V.; Keil, D.G.; Klemm, R.B. Journal of Chemical Physics, vol 83, 1985, 1630.

32. Foster, M. P.; Guillermo, R.; Galloo, J.C. International Journal of Chemical Kinetics, vol 28, 1996, 235.

33. Baxley, J.S.; Henley, M.V.; Wells, J.R. International Journal of Chemical Kinetics, vol 29, 1997, 637.

34. Kerr, J.A.; Sheppard, D.W. Environmental Science and Technology, vol 15, 1981, 960.

35. Tuazon, E.; Aschmann, S.M.; Atkinson, R.; Carter, W.P.L. Journal of Physical Chemistry A, vol 102, 1998, 2316.

36. Carter, W.P.L.; Pierce, J.A.; Malkina, I.L. Investigation of the ozone formation potential of selected volatile silicone compounds. Final Report to Dow Corning Corporation, Midland, MI, January 1992.

37. Atkinson, R.; Tuazon, E. C.; Kwok, E. S. C.; Arey, J., Aschmann, S. M.; Bridier, I.; Journal of the Chemical Society Faraday Transactions, vol 91, 1995, 3033.

38. Aschmann, S.M.; Atkinson, R. International Journal of Chemical Kinetics, vol 27, 1998, 533.

39. Atkinson, R.; Kwok, E.S.C.; Arey, J.; Aschmann, S.M. Faraday Discussions, vol 23, 1995, 23.

40. Eberhard, J.; Müller, C.; Stocker, D.W.; Kerr, J.A. Environmental Science and Technology, vol 29, 1995, 232.

41. Odum, J.R.; Jungkamp, T.P.W.; Griffin, R.J.; Flagan, R.C.; Seinfeld, J.H. Science, vol 276, 1997, 96.

42. Kwok, E.S.C.; Aschmann, S.M.; Atkinson, R. Environmental Science and Technology, vol 30, 1996, 329.